

Neutrino masses in the minimal gauged $(B - L)$ supersymmetry

Yu-Li Yan*, Tai-Fu Feng†, Jin-Lei Yang, Hai-Bin Zhang‡, Shu-Min Zhao, Rong-Fei Zhu

Department of Physics, Hebei University, Baoding, 071002, China

Abstract

We present the radiative corrections to neutrino masses in a minimal supersymmetric extension of the standard model with local $U(1)_{B-L}$ symmetry. At tree level, three tiny active neutrinos and two nearly massless sterile neutrinos can be obtained through the seesaw mechanism. Considering the one-loop corrections to the neutrino masses, the numerical results indicate that two sterile neutrinos obtain KeV masses and the small active-sterile neutrino mixing angles. The lighter sterile neutrino is a very interesting dark matter candidate in cosmology. Meanwhile the active neutrinos mixing angles and mass squared differences agree with present experimental data.

PACS numbers: 12.60.Jv, 14.60.Pq, 14.60.St

Keywords: supersymmetry, radiative corrections, neutrino mass

* yychanghe@hbu.edu.cn

† fengtf@hbu.edu.cn

‡ hbzhang@hbu.edu.cn

I. INTRODUCTION

The discovery of Higgs boson on the Large Hadron Collider (LHC) [1, 2] indicates that the Higgs mechanism to break electroweak symmetry has an experimental cornerstone now. The experiments of atmospheric and solar neutrino oscillation give the neutrino data at least three types of neutrinos which have sub-eV masses, but the standard model (SM) of particle physics cannot account for the origin of these tiny masses naturally.

Three flavor neutrinos are mixed into massive neutrinos $\nu_{1,2,3}$ during their flight, and the mixings are described by the Pontecorvo-Maki-Nakagawa-Sakata matrix U_{PMNS} [3, 4]. At one standard deviation, a global fitting from the updated neutrino oscillation experimental data gives the differences of mass squared and mixing angles as [5]

$$\begin{aligned}
 \Delta m_{\odot}^2 &= 7.54_{-0.22}^{+0.26} \times 10^{-5} \text{ eV}^2, \\
 \Delta m_A^2(\text{NO}) &= 2.43_{-0.06}^{+0.06} \times 10^{-3} \text{ eV}^2, & \Delta m_A^2(\text{IO}) &= 2.38_{-0.06}^{+0.06} \times 10^{-3} \text{ eV}^2, \\
 \sin^2 \theta_{12} &= 0.308 \pm 0.0017, \\
 \sin^2 \theta_{23}(\text{NO}) &= 0.437_{-0.023}^{+0.033}, & \sin^2 \theta_{23}(\text{IO}) &= 0.455_{-0.031}^{+0.039}, \\
 \sin^2 \theta_{13}(\text{NO}) &= 0.0234_{-0.0019}^{+0.0020}, & \sin^2 \theta_{13}(\text{IO}) &= 0.0240_{-0.0022}^{+0.0019}.
 \end{aligned} \tag{1}$$

The values correspond to neutrino mass spectrum with normal ordering (NO) or inverted ordering (IO). To account for the neutrino oscillation data in Eq. (1), a theory beyond the SM is necessary.

The supersymmetric extension of the SM is a rather popular choice. The discrete symmetry R-parity is defined through $R = (-1)^{3(B-L)+2S}$, where B , L , and S are baryon number, lepton number, and the spin of the particle, respectively [6]. In the minimal supersymmetry extension of SM (MSSM) with local $U(1)_{B-L}$ symmetry, the nonzero vacuum expectation values (VEVs) of the right-handed sneutrinos evoke the $(B-L)$ symmetry and R-parity spontaneously broken simultaneously [7–12]. At tree level, the MSSM with local $U(1)_{B-L}$ symmetry can generate three active neutrinos to interpret the neutrino oscillation through the seesaw mechanism; meanwhile, the model predicts that there are two sterile neutrinos. Nevertheless, two sterile neutrinos have far below eV masses at tree level [10–13]. Sterile neutrinos with KeV scale masses are a well-motivated dark matter candidate for two reasons.

First, fermionic dark matter cannot have an arbitrarily small mass, since in dense regions it cannot be packed within an infinitely small volume for the Pauli principle. Second, sterile neutrinos have a small mixing with the active neutrinos which would enable a dark matter particle to decay into an active neutrino and a photon [14]. The Tremaine-Gunn bound indicates that a sterile neutrino mass must be greater than about 0.4 KeV [14, 15]. A strong bound on a sterile neutrino mass and mixing angle comes from the nondetection results of the monoenergetic X-rays by the decay of sterile neutrino [14]. Recently two groups reported evidence for a 3.55 KeV emission line which could be from the decay of a 7.1 KeV sterile neutrino with $\sin^2(2\theta) \sim 10^{-10}$ or 10^{-11} [16, 17], which is just below the previous X-ray bound. This observation is being fiercely discussed [18–21].

In this work, we investigate the origin of neutrino masses in the minimal gauged ($B - L$) supersymmetry. There are five light neutrinos (three light active and two almost massless sterile neutrinos) at tree level, which agrees with the results in Refs.[10–13]. The one-loop corrections to the light neutrinos are important to account for relevant experimental data [22, 23]. In this article we present the one-loop radiative corrections to neutrino masses and relevant mixing matrix in the MSSM with local $U(1)_{B-L}$ symmetry. The numerical results indicate that there is parameter space to give two sterile neutrinos KeV masses and the small active-sterile neutrino mixing angles. The lighter sterile neutrino is a very interesting dark matter candidate in cosmology. Meanwhile, the mass squared differences and mixing angles of active neutrinos coincide with the experimental data from the solar and atmospheric oscillations [5].

Our presentation is organized as follows. In Sec. II, we briefly summarize the main ingredients of the MSSM with local $U(1)_{B-L}$ symmetry and then present the mass matrix for neutralinos and neutrinos at tree level in Sec. III. In Sec. IV, we analyze one-loop radiative corrections to the mass matrix. The numerical analysis for two possibilities on the neutrino mass spectrum (NO and IO) is given in Sec. V, and Sec. VI gives a summary.

II. THE SUPERSYMMETRIC MODEL WITH LOCAL $U(1)_{B-L}$ SYMMETRY

When $U(1)_{B-L}$ is a local gauge symmetry, one can enlarge the local gauge group of the MSSM to $SU(3)_C \otimes SU(2)_L \otimes U(1)_Y \otimes U(1)_{B-L}$. In the model proposed in Refs. [10–12], three exotic superfields for right-handed neutrinos are $\hat{N}_i^c \sim (1, 1, 0, 1)$. Meanwhile, quantum numbers of the matter chiral superfields for quarks and leptons are given by

$$\begin{aligned} \hat{Q}_I &= \begin{pmatrix} \hat{U}_I \\ \hat{D}_I \end{pmatrix} \sim \left(3, 2, \frac{1}{3}, \frac{1}{3}\right), & \hat{L}_I &= \begin{pmatrix} \hat{\nu}_I \\ \hat{E}_I \end{pmatrix} \sim (1, 2, -1, -1), \\ \hat{U}_I^c &\sim \left(3, 1, -\frac{4}{3}, -\frac{1}{3}\right), & \hat{D}_I^c &\sim \left(3, 1, \frac{2}{3}, -\frac{1}{3}\right), & \hat{E}_I^c &\sim (1, 1, 2, 1), \end{aligned} \quad (2)$$

with $I = 1, 2, 3$ denoting the index of generation. In addition, the quantum numbers of two Higgs doublets are assigned as

$$\hat{H}_u = \begin{pmatrix} \hat{H}_u^+ \\ \hat{H}_u^0 \end{pmatrix} \sim (1, 2, 1, 0), \quad \hat{H}_d = \begin{pmatrix} \hat{H}_d^0 \\ \hat{H}_d^- \end{pmatrix} \sim (1, 2, -1, 0). \quad (3)$$

The superpotential of the MSSM with local $U(1)_{B-L}$ symmetry is written as [13, 24–26]

$$\mathcal{W} = \mathcal{W}_{MSSM} + (Y_N)_{IJ} \hat{H}_u^T i\sigma_2 \hat{L}_I \hat{N}_J^c, \quad (4)$$

with \mathcal{W}_{MSSM} denoting the superpotential of the MSSM. Correspondingly, the soft breaking terms of the MSSM with local $U(1)_{B-L}$ symmetry are generally given as

$$\begin{aligned} \mathcal{L}_{soft} &= \mathcal{L}_{soft}^{MSSM} - (m_{\tilde{N}_c}^2)_{IJ} \tilde{N}_I^{c*} \tilde{N}_J^c - (m_{BL} \lambda_{BL} \lambda_{BL} + m_{BBL} \lambda_B \lambda_{BL} + H.c.) \\ &\quad + \{(A_N)_{IJ} H_u^T i\sigma_2 \tilde{L}_I \tilde{N}_J^c + H.c.\}. \end{aligned} \quad (5)$$

In this formula $\mathcal{L}_{soft}^{MSSM}$ is the soft breaking terms of the MSSM, and λ_{BL} denotes the gaugino of $U(1)_{B-L}$. After the $SU(2)_L$ doublets H_u , H_d , \tilde{L}_I , and $SU(2)_L$ singlets, \tilde{N}_I^c obtain the nonzero VEVs,

$$\begin{aligned} H_u &= \begin{pmatrix} H_u^+ \\ \frac{1}{\sqrt{2}}(v_u + H_u^0 + iP_u^0) \end{pmatrix}, & H_d &= \begin{pmatrix} \frac{1}{\sqrt{2}}(v_d + H_d^0 + iP_d^0) \\ H_d^- \end{pmatrix}, \\ \tilde{L}_I &= \begin{pmatrix} \frac{1}{\sqrt{2}}(v_{L_I} + \tilde{\nu}_{L_I} + iP_{\tilde{L}_I}^0) \\ \tilde{L}_I^- \end{pmatrix}, & \tilde{N}_I^c &= \frac{1}{\sqrt{2}}(v_{N_I} + \tilde{\nu}_{R_I} + iP_{\tilde{N}_I}^0), \end{aligned} \quad (6)$$

the R-parity is broken spontaneously, and the local gauge symmetry $SU(2)_L \otimes U(1)_Y \otimes U(1)_{B-L}$ breaks down to the electromagnetic symmetry $U(1)_e$. Then, the tree level masses of neutral and charged gauge bosons are, respectively, formulated as

$$\begin{aligned} m_Z^2 &= \frac{1}{4}(g_1^2 + g_2^2)v_{EW}^2, & m_W^2 &= \frac{1}{4}g_2^2v_{EW}^2, \\ m_{Z_{BL}}^2 &= g_{BL}^2(v_N^2 + v_{EW}^2 - v_{SM}^2), \end{aligned} \quad (7)$$

with abbreviations $v_{SM}^2 = v_u^2 + v_d^2$, $v_{EW}^2 = v_u^2 + v_d^2 + \sum_{\alpha=1}^3 v_{L_\alpha}^2$ and $v_N^2 = \sum_{\alpha=1}^3 v_{N_\alpha}^2$. In addition, g_2 , g_1 and g_{BL} denote the gauge couplings of $SU(2)_L$, $U(1)_Y$, and $U(1)_{B-L}$, respectively.

To satisfy present electroweak precision observations, we assume the mass of a neutral $U(1)_{B-L}$ gauge boson $m_{Z_{BL}} > 1\text{TeV}$, which implies $v_N > 1\text{TeV}$ when $g_{BL} < 1$ ($m_{Z_{BL}} \simeq g_{BL}v_N$) [12]. After the electroweak symmetry is broken spontaneously, the couplings between the left-handed neutrinos and neutralinos are $(1/\sqrt{2})v_{N_J}(Y_N)_{IJ}\psi_{L_I^1}\psi_{H_u^0} - g_{BL}v_{L_I}\psi_{L_I^1}(i\lambda_{BL}) - (1/2)g_1v_{L_I}\psi_{L_I^1}(i\lambda_B) + (1/2)g_2v_{L_I}\psi_{L_I^1}(i\lambda_A^3)$. Because of the TeV scale seesaw suppression, the Yukawa couplings $(Y_N)_{IJ}$ and nonzero VEVs v_{L_I} of left-handed sneutrino are sufficiently small for tiny active neutrino masses, $(Y_N)_{IJ} \leq 10^{-6}$ and $v_{L_I} \leq 10^{-3}$ GeV [10, 12]. Ignoring the terms which are negligible and assuming that the 3×3 matrices $m_{\tilde{L}}^2$, $m_{\tilde{N}^c}^2$ are real, we simplify the minimization conditions as [13]

$$\begin{aligned} v_u \{ \mu^2 + m_{H_u}^2 + \frac{g_1^2 + g_2^2}{8}(2v_u^2 - v_{EW}^2) \} - B\mu v_d &\simeq 0, \\ v_d \{ \mu^2 + m_{H_d}^2 + \frac{g_1^2 + g_2^2}{8}(2v_u^2 - v_{EW}^2) \} - B\mu v_u &\simeq 0, \\ \sum_{\alpha=1}^3 (m_{\tilde{L}}^2)_{I\alpha} v_{L_\alpha} + \frac{v_u}{\sqrt{2}} \sum_{\alpha=1}^3 (A_N)_{I\alpha} v_{N_\alpha} - \frac{\mu v_d}{\sqrt{2}} \zeta_I \\ - v_{L_I} \{ \frac{g_1^2 + g_2^2}{8}(2v_u^2 - v_{EW}^2) + \frac{m_{Z_{BL}}^2}{2} \} &\simeq 0, \\ \sum_{\alpha=1}^3 (m_{\tilde{N}^c}^2)_{I\alpha} v_{N_\alpha} + \frac{m_{Z_{BL}}^2}{2} v_{N_I} &\simeq 0, \end{aligned} \quad (8)$$

where $\zeta_I = \sum_{\alpha=1}^3 (Y_N)_{I\alpha} v_{N_\alpha}$. Note that the first two minimization conditions for H_u^0 and H_d^0 are not greatly altered from those in the MSSM, the third condition originates from the linear terms of v_{L_I} , and the last equation implies that the vector $(v_{N_1}, v_{N_2}, v_{N_3})$ is an eigenvector of 3×3 mass squared matrix $m_{\tilde{N}^c}^2$ with eigenvalue $-m_{Z_{BL}}^2/2$. Considering the

last minimization condition in Eq. (8), we formulate the symmetric 3×3 matrix as

$$m_{\tilde{N}^c}^2 = \begin{pmatrix} \xi_{\tilde{N}_1^c}^2 - m_{Z_{BL}}^2/2 & 0 & -\frac{v_{N_1}}{v_{N_3}} \xi_{\tilde{N}_1^c}^2 \\ 0 & \xi_{\tilde{N}_2^c}^2 - m_{Z_{BL}}^2/2 & -\frac{v_{N_2}}{v_{N_3}} \xi_{\tilde{N}_2^c}^2 \\ -\frac{v_{N_1}}{v_{N_3}} \xi_{\tilde{N}_1^c}^2 & -\frac{v_{N_2}}{v_{N_3}} \xi_{\tilde{N}_2^c}^2 & \frac{\xi_{\tilde{N}_1^c}^2 v_{N_1} + \xi_{\tilde{N}_2^c}^2 v_{N_2}}{v_{N_3}} - m_{Z_{BL}}^2/2 \end{pmatrix}, \quad (9)$$

with $\xi_{\tilde{N}_1^c}^2 = (m_{\tilde{N}^c}^2)_{11} + m_{Z_{BL}}^2/2$, $\xi_{\tilde{N}_2^c}^2 = (m_{\tilde{N}^c}^2)_{22} + m_{Z_{BL}}^2/2$. This is the mixing matrix of the right-handed sneutrinos, the reasons for choosing it are shown in Appendix A.

III. THE MASS MATRIX FOR NEUTRALINOS AND NEUTRINOS AT TREE LEVEL

In the MSSM with local $U(1)_{B-L}$ symmetry, the nonzero VEVs of left- and right-handed sneutrinos induce the mixing between neutralinos (charginos) and neutrinos (charged leptons). In the basis $\Psi^{0T} = (\nu_{L_I}, N_J^c, i\lambda_{BL}, i\lambda_B, i\lambda_A^3, \psi_{H_d}^1, \psi_{H_u}^2)$, we can obtain the neutral fermion mass terms in the Lagrangian

$$\mathcal{L}_{neutral}^{mass} = \frac{1}{2} \Psi^{0T} M_N \Psi^0 + H.c., \quad (10)$$

where the mass matrix for neutralinos and neutrinos M_N is given by

$$M_N = \begin{pmatrix} 0_{3 \times 3} & (\mathcal{A}_N^{(1)})_{3 \times 4} & (\mathcal{A}_N^{(2)})_{3 \times 4} \\ (\mathcal{A}_N^{(1)T})_{4 \times 3} & (\mathcal{M}_N^{(0)})_{4 \times 4} & (\mathcal{A}_N^{(3)})_{4 \times 4} \\ (\mathcal{A}_N^{(2)T})_{4 \times 3} & (\mathcal{A}_N^{(3)T})_{4 \times 4} & (\mathcal{M}_N)_{4 \times 4} \end{pmatrix}, \quad (11)$$

where \mathcal{M}_N denotes the 4×4 mass matrix for neutralinos in the MSSM. The concrete expressions for $\mathcal{M}_N^{(0)}$, $\mathcal{A}_N^{(1)}$, $\mathcal{A}_N^{(2)}$, and $\mathcal{A}_N^{(3)}$ are

$$\mathcal{M}_N^{(0)} = \begin{pmatrix} 0_{3 \times 3} & (g_{BL} v_{N_J})_{3 \times 1} \\ (g_{BL} v_{N_{J'}})_{1 \times 3} & 2m_{BL} \end{pmatrix},$$

$$\mathcal{A}_N^{(1)} = \begin{pmatrix} (v_{N_I} Y_N)_{IJ'}_{3 \times 3} & (-g_{BL} v_{L_I})_{3 \times 1} \end{pmatrix},$$

$$\mathcal{A}_N^{(2)} = \begin{pmatrix} (-\frac{g_1}{2} v_{L_I})_{3 \times 1} & (\frac{g_2}{2} v_{L_I})_{3 \times 1} & 0_{3 \times 1} & (\frac{\zeta_I}{\sqrt{2}})_{3 \times 1} \end{pmatrix},$$

$$\mathcal{A}_N^{(3)} = \begin{pmatrix} 0_{3 \times 1} & 0_{3 \times 1} & 0_{3 \times 1} & (\frac{1}{\sqrt{2}} \sum_{\alpha=1}^3 v_{L\alpha} (Y_N)_{\alpha J})_{3 \times 1} \\ m_{BBL} & 0 & 0 & 0 \end{pmatrix}, \quad (12)$$

with the row indices of matrix $I, J = 1, 2, 3$ and the column indices of matrix $I', J' = 1, 2, 3$, respectively. The eigenvalues of the 4×4 mass matrix $\mathcal{M}_N^{(0)}$ are given as

$$m_{N_1} = m_{N_2} = 0, \quad m_{N_3} = m_{BL} - \Delta_{BL}, \quad m_{N_4} = m_{BL} + \Delta_{BL}, \quad (13)$$

where $\Delta_{BL} = \sqrt{m_{BL}^2 + g_{BL}^2 v_N^2}$, and then we can obtain $m_{N_{3,4}}$ about TeV region for $m_{ZBL} > 1\text{TeV}$ ($m_{ZBL} \simeq g_{BL} v_N$). The matrix $\mathcal{M}_N^{(0)}$ has four eigenvalues which are zero order approximations of the $U(1)_{B-L}$ gaugino and three right-handed neutrinos masses. However, there are only two nonzero eigenvalues, and the other two eigenvalues are zero.

Defining the 4×4 orthogonal matrix

$$U_N = \begin{pmatrix} -\frac{v_{N_3}}{\sqrt{v_{N_1}^2 + v_{N_3}^2}} & -\frac{v_{N_1} v_{N_2}}{v_N \sqrt{v_{N_1}^2 + v_{N_3}^2}} & -\frac{g_{BL} v_{N_1}}{\sqrt{2} \Delta_{BL} \eta_{BL}^-} & \frac{g_{BL} v_{N_1}}{\sqrt{2} \Delta_{BL} \eta_{BL}^+} \\ 0 & \frac{\sqrt{v_{N_1}^2 + v_{N_3}^2}}{v_N} & -\frac{g_{BL} v_{N_2}}{\sqrt{2} \Delta_{BL} \eta_{BL}^-} & \frac{g_{BL} v_{N_2}}{\sqrt{2} \Delta_{BL} \eta_{BL}^+} \\ \frac{v_{N_1}}{\sqrt{v_{N_1}^2 + v_{N_3}^2}} & -\frac{v_{N_3} v_{N_2}}{v_N \sqrt{v_{N_1}^2 + v_{N_3}^2}} & -\frac{g_{BL} v_{N_3}}{\sqrt{2} \Delta_{BL} \eta_{BL}^-} & \frac{g_{BL} v_{N_3}}{\sqrt{2} \Delta_{BL} \eta_{BL}^+} \\ 0 & 0 & \frac{1}{\sqrt{2}} \eta_{BL}^- & \frac{1}{\sqrt{2}} \eta_{BL}^+ \end{pmatrix}, \quad (14)$$

one obtains

$$\begin{aligned} M &= \begin{pmatrix} 1_{3 \times 3} & 0_{3 \times 4} & 0_{3 \times 4} \\ 0_{4 \times 3} & (U_N^T)_{4 \times 4} & 0_{4 \times 4} \\ 0_{4 \times 3} & 0_{4 \times 4} & 1_{4 \times 4} \end{pmatrix} \cdot M_N \cdot \begin{pmatrix} 1_{3 \times 3} & 0_{3 \times 4} & 0_{3 \times 4} \\ 0_{4 \times 3} & (U_N)_{4 \times 4} & 0_{4 \times 4} \\ 0_{4 \times 3} & 0_{4 \times 4} & 1_{4 \times 4} \end{pmatrix} \\ &= \begin{pmatrix} 0_{3 \times 3} & (\mathcal{A}_N^{(1)} U_N)_{3 \times 4} & (\mathcal{A}_N^{(2)})_{3 \times 4} \\ (U_N^T \mathcal{A}_N^{(1)T})_{4 \times 3} & (U_N^T \mathcal{M}_N^{(0)} U_N)_{4 \times 4} & (U_N^T \mathcal{A}_N^{(3)})_{4 \times 4} \\ (\mathcal{A}_N^{(2)T})_{4 \times 3} & (\mathcal{A}_N^{(3)T} U_N)_{4 \times 4} & (\mathcal{M}_N)_{4 \times 4} \end{pmatrix} \\ &= \begin{pmatrix} (m_\nu)_{5 \times 5} & (m_D)_{5 \times 6} \\ (m_D^T)_{6 \times 5} & (\mathcal{M})_{6 \times 6} \end{pmatrix}, \end{aligned} \quad (15)$$

where $\eta_{BL}^\pm = \sqrt{1 \pm \frac{m_{BL}}{\Delta_{BL}}}$, and $U_N^T \mathcal{M}_N^{(0)} U_N = \text{diag}(0, 0, m_{BL} - \Delta_{BL}, m_{BL} + \Delta_{BL})$, respectively.

Using Eqs. (11) and (14), we formulate the submatrices in Eq. (15), respectively, as

$$\begin{aligned}
m_\nu &= \begin{pmatrix} 0_{3 \times 3} & \delta_{i3} & \delta_{i2} \\ \delta_{i3} & 0 & 0 \\ \delta_{i2} & 0 & 0 \end{pmatrix}, & m_D &= \begin{pmatrix} -\delta_i^- & \delta_i^+ & -\frac{g_1}{2}v_{L_i} & \frac{g_2}{2}v_{L_i} & 0_{3 \times 1} & \frac{1}{\sqrt{2}}\zeta_i \\ 0 & 0 & 0 & 0 & 0 & \varepsilon_{13} \\ 0 & 0 & 0 & 0 & 0 & \varepsilon_{12} \end{pmatrix}, \\
\mathcal{M} &= \begin{pmatrix} m_{BL} - \Delta_{BL} & 0 & \frac{1}{\sqrt{2}}\eta^- m_{BBL} & 0 & 0 & -\varepsilon_- \\ 0 & m_{BL} + \Delta_{BL} & \frac{1}{\sqrt{2}}\eta^+ m_{BBL} & 0 & 0 & \varepsilon_+ \\ \frac{1}{\sqrt{2}}\eta^- m_{BBL} & \frac{1}{\sqrt{2}}\eta^+ m_{BBL} & M_1 & 0 & -\frac{g_1}{2}v_d & \frac{g_1}{2}v_u \\ 0 & 0 & 0 & M_2 & \frac{g_2}{2}v_d & -\frac{g_2}{2}v_u \\ 0 & 0 & -\frac{g_1}{2}v_d & \frac{g_2}{2}v_d & 0 & -\mu \\ -\varepsilon_- & \varepsilon_+ & \frac{g_1}{2}v_u & -\frac{g_2}{2}v_u & -\mu & 0 \end{pmatrix}, & (16)
\end{aligned}$$

where the abbreviations are

$$\begin{aligned}
\varepsilon_N^2 &= \sum_{\alpha, \beta=1}^3 v_{L_\alpha} (Y_N)_{\alpha\beta} v_{N_\beta}, & \varepsilon_\pm &= \frac{g_{BL} \varepsilon_N^2}{2\Delta_{BL} \eta_{BL}^\pm}, \\
\delta_i^\pm &= \frac{g_{BL} v_u}{2\Delta_{BL} \eta_{BL}^\pm} \zeta_i \mp \frac{1}{\sqrt{2}} g_{BL} \eta_{BL}^\pm v_{L_i}, \\
\delta_{i2} &= \frac{v_u}{\sqrt{2}(v_{N_1}^2 + v_{N_3}^2)} [-(Y_N)_{i1} v_{N_1} v_{N_2} + (Y_N)_{i2} (v_{N_1}^2 + v_{N_3}^2) - (Y_N)_{i3} v_{N_2} v_{N_3}], \\
\delta_{i3} &= \frac{v_u}{v_N \sqrt{2}(v_{N_1}^2 + v_{N_3}^2)} [-(Y_N)_{i1} v_{N_3} + (Y_N)_{i3} v_{N_1}], \\
\varepsilon_{12} &= \frac{1}{v_u} \sum_{\alpha=1}^3 v_{L_\alpha} \delta_{\alpha 2}, & \varepsilon_{13} &= \frac{1}{v_u} \sum_{\alpha=1}^3 v_{L_\alpha} \delta_{\alpha 3}, & (17)
\end{aligned}$$

with the indices $i = 1, 2, 3$. The abbreviations are suppressed by the tiny $(Y_N)_{ij}$ and v_{L_i} , and they are very small.

Defining the 11×11 approximated orthogonal transformation matrix \mathcal{Z}_N [13]

$$\mathcal{Z}_N = \begin{pmatrix} [1 - \frac{1}{2}m_D \cdot \mathcal{M}^{-2} \cdot m_D^T]_{5 \times 5} & [m_D \cdot \mathcal{M}^{-1} + m_\nu \cdot m_D \cdot \mathcal{M}^{-2}]_{5 \times 6} \\ -[\mathcal{M}^{-1} \cdot m_D^T + \mathcal{M}^{-2} \cdot m_D^T \cdot m_\nu]_{6 \times 5} & [1 - \frac{1}{2}\mathcal{M}^{-1} \cdot m_D^T \cdot m_D \cdot \mathcal{M}^{-1}]_{6 \times 6} \end{pmatrix}, \quad (18)$$

via the seesaw mechanism, we finally write the effective mass matrix for five light neutrinos (three active and two sterile) as

$$\begin{aligned}
m_{eff} &\simeq m_\nu - m_D \cdot \mathcal{M}^{-1} \cdot m_D^T - \frac{1}{2}m_\nu \cdot m_D \cdot \mathcal{M}^{-2} \cdot m_D^T - \frac{1}{2}m_D \cdot \mathcal{M}^{-2} \cdot m_D^T \cdot m_\nu \\
&\simeq \begin{pmatrix} [M_\nu^{LL}]_{3 \times 3} & [M_\nu^{LR}]_{3 \times 2} \\ [M_\nu^{LR,T}]_{2 \times 3} & [M_\nu^{RR}]_{2 \times 2} \end{pmatrix}, & (19)
\end{aligned}$$

where M_ν^{LL} is the three active Majorana mass matrices, M_ν^{LR} is the Dirac mixing mass matrix and M_ν^{RR} is the two sterile Majorana mass matrices. The concrete expression of M_ν^{LL} , M_ν^{LR} , and M_ν^{RR} can be found in Appendix B. From Eqs. (B2) and (17) the elements of M_ν^{RR} are related to the square of tiny $(Y_N)_{ij}v_{L_i}$; therefore, they are almost zero. The two sterile neutrinos are almost massless at tree level.

In order to accommodate naturally the experimental data on neutrino oscillation and Z invisible decay width in this framework, one can find that only one possibility $M_\nu^{LL} \gg M_\nu^{LR}$, M_ν^{RR} is reasonable [10]. In fact, from Eq. (B2) this point implies

$$\delta_{i2}, \delta_{i3} \ll \frac{v_{L_i}^2}{\Lambda_\nu} + \frac{\zeta_i^2}{\Lambda_\zeta} + \frac{2v_{L_i}\zeta_i}{\Lambda_{\nu\zeta}}. \quad (20)$$

To guarantee the decoupling of two tiny sterile neutrinos from the active neutrinos, we choose the Yukawa coupling for right-handed neutrinos as

$$Y_N = \frac{1}{v_N} \begin{pmatrix} v_{N_1}Y_1 & v_{N_2}Y_1 & v_{N_3}Y_1 \\ v_{N_1}Y_2 & v_{N_2}Y_2 & v_{N_3}Y_2 \\ v_{N_1}Y_3 & v_{N_2}Y_3 & v_{N_3}Y_3 \end{pmatrix} = \frac{1}{v_N} \begin{pmatrix} Y_1 & 0 & 0 \\ 0 & Y_2 & 0 \\ 0 & 0 & Y_3 \end{pmatrix} \begin{pmatrix} v_{N_1} & v_{N_2} & v_{N_3} \\ v_{N_1} & v_{N_2} & v_{N_3} \\ v_{N_1} & v_{N_2} & v_{N_3} \end{pmatrix}, \quad (21)$$

then we get $\zeta_i = Y_i v_N$, $\delta_{i2} = \delta_{i3} = 0$, ($i = 1, 2, 3$).

Only including the tree level contributions to the light neutrino mass matrix in Eq. (19), we diagonalize the effective neutrino mass matrix m_{eff} and then obtain three light left-handed neutrinos and two nearly massless sterile neutrinos [10–13]. Recently, it has been shown in Refs. [14, 16, 17] that sterile neutrinos with KeV scale masses are interesting dark matter candidates in the Universe. The one-loop radiative corrections are important, especially for the light neutrinos [27, 28]. We consider the one-loop radiative corrections to the mass matrix of the neutrinos in Eq. (15) and expect that two sterile neutrinos acquire their physical masses at KeV level in the following.

IV. THE RADIATIVE CORRECTIONS ON MASSES OF NEUTRINOS

A. The radiative corrections on masses of sterile neutrinos

In this model, there is a large mixing between three right-handed neutrinos and a $(B-L)$ gaugino. At leading order, this mixing induces two heavy Majorana fermions with masses

about TeV scale and two light sterile neutrinos which acquire their tiny masses by a seesaw mechanism. Here, we consider one-loop radiative corrections to the masses of two light sterile neutrinos. From interactions of the gauge and matter multiplets $ig\sqrt{2}T_{ij}^2(\lambda^a\psi_j A_i^* - \bar{\lambda}^a\bar{\psi}_i A_j)$, $-gT_{ij}^a V_\mu^a \bar{\psi}_i \bar{\sigma}^\mu \psi_j$ [30], we can obtain the couplings involving sterile neutrinos. In the Majorana case, the most general form for $N_\alpha \rightarrow N_\beta$ transition reads

$$\Sigma_{\alpha\beta}(\not{p}) = \Sigma_{\alpha\beta}^L(p^2)\not{p}P_L + \Sigma_{\alpha\beta}^{L*}(p^2)\not{p}P_R + \Sigma_{\alpha\beta}^M(p^2)P_L + \Sigma_{\alpha\beta}^{M*}(p^2)P_R. \quad (22)$$

The invariance of CPT transformation requires

$$\begin{aligned} \Sigma_{\alpha\beta}^L(p^2) &= \Sigma_{\beta\alpha}^{L*}(p^2), \\ \Sigma_{\alpha\beta}^M(p^2) &= \Sigma_{\beta\alpha}^{M*}(p^2). \end{aligned} \quad (23)$$

The radiative corrections from real and image components of scalar right-handed neutrinos are

$$\begin{aligned} \Sigma_{\alpha\beta}^{L(1)}(p^2) &= \frac{2g_{BL}^2}{(4\pi)^2} \sum_{\delta=1}^4 \sum_{i,j}^3 (U_N)_{i\alpha}^* (U_N)_{4\delta}^* (U_N)_{j\delta} (U_N)_{4\beta} \\ &\quad \times \left[\sum_{a=1}^3 (U_{\tilde{N}_E})_{ia} (U_{\tilde{N}_E})_{ja} B_1(p^2, m_{N_\delta}^2, m_{H_{N_a}}^2) \right. \\ &\quad \left. + \sum_{a=1}^3 (U_{\tilde{N}_O})_{ia} (U_{\tilde{N}_O})_{ja} B_1(p^2, m_{N_\delta}^2, m_{P_{N_a}}^2) \right], \\ \Sigma_{\alpha\beta}^{M(1)}(p^2) &= \frac{2g_{BL}^2}{(4\pi)^2} \sum_{\delta=1}^4 \sum_{i,j}^3 m_{N_\delta} (U_N)_{i\alpha} (U_N)_{4\delta} (U_N)_{j\delta} (U_N)_{4\beta} \\ &\quad \times \left[\sum_{a=1}^3 (U_{\tilde{N}_E})_{ia} (U_{\tilde{N}_E})_{ja} B_0(p^2, m_{N_\delta}^2, m_{H_{N_a}}^2) \right. \\ &\quad \left. - \sum_{a=1}^3 (U_{\tilde{N}_O})_{ia} (U_{\tilde{N}_O})_{ja} B_0(p^2, m_{N_\delta}^2, m_{P_{N_a}}^2) \right]. \end{aligned} \quad (24)$$

where $U_{\tilde{N}_O}$, $U_{\tilde{N}_E}$ can be found in Appendix B, and U_N is given in Eq. (14).

In a similar way, the radiative corrections from a $(B - L)$ gauge boson are written as

$$\begin{aligned} \Sigma_{\alpha\beta}^{L(2)}(p^2) &= \frac{g_{BL}^2}{2(4\pi)^2} \sum_{\delta=1}^4 \sum_{i,j}^3 (U_N)_{i\alpha}^* (U_N)_{i\delta} (U_N)_{j\delta}^* (U_N)_{j\beta} \left(B_1(p^2, m_{N_\delta}^2, m_{Z_{BL}}^2) - \frac{1}{2} \right), \\ \Sigma_{\alpha\beta}^{M(2)}(p^2) &= \frac{g_{BL}^2}{(4\pi)^2} \sum_{\delta=1}^4 \sum_{i,j}^3 m_{N_\delta} (U_N)_{i\alpha} (U_N)_{i\delta}^* (U_N)_{j\delta}^* (U_N)_{j\beta} \left(B_0(p^2, m_{N_\delta}^2, m_{Z_{BL}}^2) - \frac{1}{2} \right). \end{aligned} \quad (25)$$

B_0 and B_1 are two-point scalar functions. The definitions are

$$\begin{aligned} B_0(p^2, m_1^2, m_2^2) &= \frac{(2\pi\Lambda)^{2\varepsilon}}{i\pi^2} \int \frac{d^D q}{(q^2 - m_1^2)((q-p)^2 - m_2^2)}, \\ p_\mu B_1(p^2, m_1^2, m_2^2) &= \frac{(2\pi\Lambda)^{2\varepsilon}}{i\pi^2} \int \frac{d^D q q_\mu}{(q^2 - m_1^2)((q-p)^2 - m_2^2)}, \end{aligned} \quad (26)$$

with $\varepsilon = 2 - \frac{D}{2}$, where Λ denotes the energy scale of new physics, and $\Lambda = 2$ TeV in our numerical analysis.

The generic expression for the right-handed Majorana neutrinos and the $(B-L)$ gaugino self-energy must be symmetric in its indices α, β , and the result of one-loop corrections to the mass matrix in the modified dimensional reduction (\overline{DR}) scheme [22] is written as

$$\begin{aligned} (\Delta\mathcal{M}_N^{(0)})_{\alpha\beta} &= \frac{1}{2} [\mathcal{R}(\hat{\Sigma}_{\alpha\beta}^M(m_{N_\alpha}^2)) + \mathcal{R}(\hat{\Sigma}_{\beta\alpha}^M(m_{N_\beta}^2)) \\ &\quad - m_{N_\alpha} \mathcal{R}(\hat{\Sigma}_{\alpha\beta}^L(m_{N_\alpha}^2)) - m_{N_\beta} \mathcal{R}(\hat{\Sigma}_{\beta\alpha}^L(m_{N_\beta}^2))], \end{aligned} \quad (27)$$

where $\hat{\Sigma}$ denotes the renormalized self-energy in the \overline{DR} scheme.

Using the concrete expression of U_N in Eq. (14) ($(U_N)_{41} = (U_N)_{42} = 0$) and the fact $m_{N_{1,2}} \ll m_{N_{3,4}}$ in Eq. (13), when $\alpha, \beta \leq 2$, we find

$$\hat{\Sigma}_{\alpha\beta}^L(p^2) = \hat{\Sigma}_{\alpha\beta}^{L(2)}(p^2), \quad \hat{\Sigma}_{\alpha\beta}^M(p^2) = \hat{\Sigma}_{\alpha\beta}^{M(2)}(p^2), \quad (28)$$

then

$$\begin{aligned} (\Delta\mathcal{M}_N^{(0)})_{\alpha\beta} &= \frac{g_{BL}^2}{2(4\pi)^2} \sum_{\delta=3}^4 \sum_{i,j}^3 m_{N_\delta} [\mathcal{R}((U_N)_{i\alpha}(U_N)_{i\delta}^*(U_N)_{j\delta}^*(U_N)_{j\beta}) + (\alpha \leftrightarrow \beta)] \\ &\quad \times (\hat{B}_0(m_{N_\alpha}^2, m_{N_\delta}^2, m_{Z_{BL}}^2) - \frac{1}{2}), \end{aligned} \quad (29)$$

where two-point scalar functions B_0 and B_1 are renormalized in the \overline{DR} scheme, denoted by \hat{B}_0 and \hat{B}_1 , respectively. The corrections to the masses of sterile neutrino have nothing to do with small $(Y_N)_{ij}$ and v_{L_i} . As $\alpha = 1, 2, \beta = 3, 4$ and $\alpha, \beta = 3, 4$, the results of one-loop corrections to the mass matrix can be found in Appendix C.

B. The radiative corrections on masses of three active neutrinos

Generally the interaction between the left-handed neutrino and neutralinos, $(B-L)$ gaugino and charginos also induces the radiative corrections to the masses of left-handed

neutrinos. However, these corrections are suppressed by the tiny Yukawa Couplings $(Y_N)_{ij}$ and VEVs v_{L_i} of the left-handed sneutrino. The results of one-loop radiative corrections to three active neutrinos [29, 31] are

$$\begin{aligned}
(\Delta \mathcal{M}_L^{(0)})_{ij} &= \frac{\alpha_{EW} \delta(m_{\tilde{\nu}}^2)_{LL}^{ij}}{4\pi s_W^2 c_W^2 \Lambda^2} \sum_{\alpha=1}^4 (c_W(U_{\chi^0})_{2\alpha} - s_W(U_{\chi^0})_{1\alpha}) m_{\chi_\alpha^0} \varrho_{1,1}(x_{\chi_\alpha^0}, x_{\tilde{\nu}_{L_i}}, x_{\tilde{\nu}_{L_j}}) \\
&+ \frac{\alpha_{BL} \delta(m_{\tilde{\nu}}^2)_{LL}^{ij}}{2\pi \Lambda^2} \sum_{\alpha=3}^4 (U_N)_{4\alpha} m_{N_\alpha} \varrho_{1,1}(x_{N_\alpha}, x_{\tilde{\nu}_{L_i}}, x_{\tilde{\nu}_{L_j}}) \\
&+ \frac{\alpha_{EW} \delta(m_{\tilde{e}}^2)_{LL}^{ij}}{2\pi s_W^2 \Lambda^2} \sum_{\alpha=1}^2 (U_\pm)_{1\alpha}^2 m_{\chi_\alpha^\pm} \varrho_{1,1}(x_{\chi_\alpha^\pm}, x_{\tilde{e}_{L_i}}, x_{\tilde{e}_{L_j}}) \\
&- \frac{\alpha_{EW} \mu^2 \zeta_i \zeta_j}{16\pi s_W^2 c_W^2 s_\beta^2 \Lambda^4} \sum_{\alpha=1}^4 (c_W(U_{\chi^0})_{2\alpha} - s_W(U_{\chi^0})_{1\alpha}) m_{\chi_\alpha^0} \\
&\times \{ \cos^2(\alpha - \beta) \varrho_{1,1}(x_{\chi_\alpha^0}, x_{\tilde{\nu}_{L_i}}, x_{\tilde{\nu}_{L_j}}, x_h) \\
&+ \sin^2(\alpha - \beta) \varrho_{1,1}(x_{\chi_\alpha^0}, x_{\tilde{\nu}_{L_i}}, x_{\tilde{\nu}_{L_j}}, x_H) - \varrho_{1,1}(x_{\chi_\alpha^0}, x_{\tilde{\nu}_{L_i}}, x_{\tilde{\nu}_{L_j}}, x_A) \} \\
&- \frac{\alpha_{BL} \mu^2 \zeta_i \zeta_j}{4\pi s_\beta^2 \Lambda^4} \sum_{\alpha=3}^4 (U_N)_{4\alpha}^2 m_{N_\alpha} \{ \cos^2(\alpha - \beta) \varrho_{1,1}(x_{N_\alpha}, x_{\tilde{\nu}_{L_i}}, x_{\tilde{\nu}_{L_j}}, x_h) \\
&+ \sin^2(\alpha - \beta) \varrho_{1,1}(x_{N_\alpha}, x_{\tilde{\nu}_{L_i}}, x_{\tilde{\nu}_{L_j}}, x_H) - \varrho_{1,1}(x_{N_\alpha}, x_{\tilde{\nu}_{L_i}}, x_{\tilde{\nu}_{L_j}}, x_A) \} \\
&- \frac{\alpha_{EW} \mu^2 \zeta_i \zeta_j}{4\pi s_W^2 s_\beta^2 \Lambda^4} \sum_{\alpha=1}^2 (U_\pm)_{1\alpha} m_{\chi_\alpha^\pm} \varrho_{1,1}(x_{\chi_\alpha^\pm}, x_{\tilde{e}_{L_i}}, x_{\tilde{e}_{L_j}}, x_{H_\pm}), \tag{30}
\end{aligned}$$

with $\alpha_{EW} = e^2/4\pi$, $\alpha_{BL} = g_{BL}^2/4\pi$ and $\delta(m_{\tilde{\nu}}^2)_{LL}^{ij} = (\frac{g_1^2 + g_2^2}{4} + g_{BL}^2) v_{L_i} v_{L_j} + \frac{1}{2} \zeta_i \zeta_j + \frac{1}{2} (Y_N Y_N^T)_{ij} v_u^2$. Here, U_{χ^0} denotes the orthogonal matrix of a neutralino mass matrix, and U_\pm denotes the orthogonal matrix of a chargino mass matrix in the MSSM. We also adopt the abbreviations $\tan \beta = v_u / \sqrt{v_d^2 + \sum_{\alpha=1}^3 v_{L_\alpha}^2}$, $\tan 2\alpha = \frac{m_A^2 + m_Z^2}{m_A^2 - m_Z^2} \tan 2\beta$, $s_\beta^2 = \sin^2 \beta$, $s_W^2 = \sin^2 \theta_W$, and $c_W^2 = \cos^2 \theta_W$, where θ_W is the Weinberg angle. Here the functions $\varrho_{m,n}(x_1, x_2, \dots, x_N)$ are defined by

$$\varrho_{m,n}(x_1, x_2, \dots, x_N) = \sum_{i=1}^N \frac{x_i^m \ln^n x_i}{\prod_{j \neq i} (x_i - x_j)}, \tag{31}$$

with $x_i = m_i^2/\Lambda^2$.

Similarly, we derive the corrections from virtual sneutrino-neutralino to the mixing matrix $\mathcal{A}_N^{(2)}$ at a one-loop level as [29, 31]

$$\Delta \mathcal{A}_N^{(2)} = \sum_{k=1}^4 (N_F^{(2)})_{ik} \{ (s_\alpha(U_{\chi^0})_{3k} + c_\alpha(U_{\chi^0})_{4k}) s_W, -(s_\alpha(U_{\chi^0})_{3k} + c_\alpha(U_{\chi^0})_{4k}) c_W,$$

$$\begin{aligned}
& -(c_W(U_{\chi^0})_{2k} - s_W(U_{\chi^0})_{1k})s_\alpha, \quad -(c_W(U_{\chi^0})_{2k} - s_W(U_{\chi^0})_{1k})c_\alpha \varrho_{1,1}(m_{\chi_k^0}, x_h, x_{\tilde{\nu}_i}) \cos(\alpha - \beta) \\
& + (-(c_\alpha(U_{\chi^0})_{3k} + s_\alpha(U_{\chi^0})_{4k})s_W, \quad (c_\alpha(U_{\chi^0})_{3k} - s_\alpha(U_{\chi^0})_{4k})c_W, \\
& (c_W(U_{\chi^0})_{2k} - s_W(U_{\chi^0})_{1k})c_\alpha, \quad -(c_W(U_{\chi^0})_{2k} - s_W(U_{\chi^0})_{1k})s_\alpha \varrho_{1,1}(m_{\chi_k^0}, x_H, x_{\tilde{\nu}_i}) \sin(\alpha - \beta) \\
& + ((-s_\beta(U_{\chi^0})_{3k} + c_\beta(U_{\chi^0})_{4k})s_W, \quad (s_\beta(U_{\chi^0})_{3k} - c_\beta(U_{\chi^0})_{4k})c_W, \\
& -(c_W(U_{\chi^0})_{2k} - s_W(U_{\chi^0})_{1k})c_\beta, \quad -(c_W(U_{\chi^0})_{2k} - s_W(U_{\chi^0})_{1k})s_\beta \varrho_{1,1}(m_{\chi_k^0}, x_A, x_{\tilde{\nu}_i})\}, \quad (32)
\end{aligned}$$

with $s_\alpha^2 = \sin^2 \alpha$, $c_\alpha^2 = \cos^2 \alpha$, and $(N_F^{(2)})_{ik} = \frac{\alpha_{EW} \mu \zeta_i}{16\sqrt{2}\pi s_W^2 c_W^2 s_\beta \Lambda^2} (c_W(U_{\chi^0})_{2k} - s_W(U_{\chi^0})_{1k}) m_{\chi_k^0}$. Additionally, the radiative corrections to the mixing between left- and right-handed neutrinos are proportional to $Y_N \nu_{L_i}$ or $A_N \nu_{L_i}$ and can be ignored safely.

Considering those one-loop corrections, the mass matrix in Eq. (15) is rewritten as

$$\begin{aligned}
M' &= \begin{pmatrix} (\Delta \mathcal{M}_L^{(0)})_{3 \times 3} & (\mathcal{A}_N^{(1)} U_N)_{3 \times 4} & (\mathcal{A}_N^{(2)})_{3 \times 4} + \Delta \mathcal{A}_N^{(2)} \\ (U_N^T \mathcal{A}_N^{(1)T})_{4 \times 3} & (U_N^T \mathcal{M}_N^{(0)} U_N)_{4 \times 4} + (\Delta \mathcal{M}_N^{(0)})_{4 \times 4} & (U_N^T \mathcal{A}_N^{(3)})_{4 \times 4} \\ (\mathcal{A}_N^{(2)T})_{4 \times 3} & (\mathcal{A}_N^{(3)T} U_N)_{4 \times 4} & (\mathcal{M}_N)_{4 \times 4} \end{pmatrix} \\
&= \begin{pmatrix} (m_\nu + \Delta(m_\nu))_{5 \times 5} & (m_D + \Delta(m_D))_{5 \times 6} \\ (m_D + \Delta(m_D))_{6 \times 5}^T & (\mathcal{M} + \Delta(\mathcal{M}))_{6 \times 6} \end{pmatrix}. \quad (33)
\end{aligned}$$

Using the seesaw mechanism, the effective mass matrix for five light neutrinos (three active and two sterile) at the one-loop level is

$$\begin{aligned}
m'_{eff} &\simeq (m_\nu + \Delta(m_\nu)) - (m_D + \Delta(m_D)) \cdot (\mathcal{M} + \Delta(\mathcal{M}))^{-1} \cdot (m_D + \Delta(m_D))^T \\
&\quad - \frac{1}{2} (m_\nu + \Delta(m_\nu)) \cdot (m_D + \Delta(m_D)) \cdot (\mathcal{M} + \Delta(\mathcal{M}))^{-2} \cdot (m_D + \Delta(m_D))^T \\
&\quad - \frac{1}{2} (m_D + \Delta(m_D)) \cdot (\mathcal{M} + \Delta(\mathcal{M}))^{-2} \cdot (m_D + \Delta(m_D))^T \cdot (m_\nu + \Delta(m_\nu)) \\
&\simeq \begin{pmatrix} [M'_\nu{}^{LL}]_{3 \times 3} & [M'_\nu{}^{LR}]_{3 \times 2} \\ [M'_\nu{}^{LR}]_{2 \times 3}^T & [M'_\nu{}^{RR}]_{2 \times 2} \end{pmatrix}. \quad (34)
\end{aligned}$$

We can obtain five eigenvalues by diagonalizing the effective mass matrix m'_{eff} . The corrections to the sterile neutrinos are much larger than the corrections to the active neutrinos which are suppressed by the tiny parameters, so the three light eigenvalues are active neutrinos, and other two relatively heavy eigenvalues are sterile neutrinos. Under the assumption $[M'_\nu{}^{RR}] \gg [M'_\nu{}^{LL}]$, the corrected effective mass matrix of three left-handed neutrinos is

$$m'_{\nu_L}{}^{eff} \simeq M'_\nu{}^{LL}. \quad (35)$$

Using the "top-down" method [32, 33] in the effective mass matrix m'_{ν_L} , we diagonalize the Hermitian matrix

$$\mathcal{H} = (m'_{\nu_L})^\dagger m'_{\nu_L}. \quad (36)$$

The eigenvalues of the 3×3 effective mass squared matrix \mathcal{H} are given as

$$\begin{aligned} m_1^2 &= \frac{a}{3} - \frac{1}{3}p(\cos \phi + \sqrt{3} \sin \phi), \\ m_2^2 &= \frac{a}{3} - \frac{1}{3}p(\cos \phi - \sqrt{3} \sin \phi), \\ m_3^2 &= \frac{a}{3} + \frac{2}{3}p \cos \phi. \end{aligned} \quad (37)$$

To formulate the expressions of a concise form, one can define the notations

$$\begin{aligned} p &= \sqrt{a^2 - 3b}, \quad \phi = \frac{1}{3} \arccos\left(\frac{1}{p^3}\left(a^3 - \frac{9}{2}ab + \frac{27}{2}c\right)\right), \quad a = \text{Tr}(\mathcal{H}), \\ b &= \mathcal{H}_{11}\mathcal{H}_{22} + \mathcal{H}_{11}\mathcal{H}_{33} + \mathcal{H}_{22}\mathcal{H}_{33} - \mathcal{H}_{12}^2 - \mathcal{H}_{13}^2 - \mathcal{H}_{23}^2, \quad c = \text{Det}(\mathcal{H}). \end{aligned} \quad (38)$$

For the three active neutrino mixing, there are two possible solutions on the neutrino mass spectrum. The normal ordering (NO) spectrum is

$$\begin{aligned} m_{\nu_1} &< m_{\nu_2} < m_{\nu_3}, \quad m_{\nu_1}^2 = m_1^2, \quad m_{\nu_2}^2 = m_2^2, \quad m_{\nu_3}^2 = m_3^2, \\ \Delta m_{\odot}^2 &= m_{\nu_2}^2 - m_{\nu_1}^2, \quad \Delta m_A^2 = m_{\nu_3}^2 - m_{\nu_1}^2, \end{aligned} \quad (39)$$

and the neutrino mass spectrum with the inverted ordering (IO) is

$$\begin{aligned} m_{\nu_3} &< m_{\nu_1} < m_{\nu_2}, \quad m_{\nu_3}^2 = m_1^2, \quad m_{\nu_1}^2 = m_2^2, \quad m_{\nu_2}^2 = m_3^2, \\ \Delta m_{\odot}^2 &= m_{\nu_2}^2 - m_{\nu_1}^2, \quad \Delta m_A^2 = m_{\nu_2}^2 - m_{\nu_3}^2. \end{aligned} \quad (40)$$

From the mass squared matrix \mathcal{H} and three eigenvalues one can get the orthogonal matrix U_ν of \mathcal{H} [32, 33]. Correspondingly, the mixing angles among three active neutrinos are determined by

$$\sin \theta_{13} = |(U_\nu)_{13}|, \quad \sin \theta_{23} = \frac{|(U_\nu)_{23}|}{\sqrt{1 - |(U_\nu)_{13}|^2}}, \quad \sin \theta_{12} = \frac{|(U_\nu)_{12}|}{\sqrt{1 - |(U_\nu)_{13}|^2}}. \quad (41)$$

It is important to calculate the active-sterile neutrino mixing angles which are strongly constrained by X-ray observations [14]. There are several mixing angles $\theta_{\sigma I}$, where I is the

sterile neutrino flavor and σ is the active neutrino flavor. We define $\theta_{\sigma I}^2 = (M_{\nu}^{LR})_{\sigma I}^2/m_{rI}^2$, where m_{rI}^2 are the sterile neutrino masses. There are two sterile neutrinos; then, $I = 1, 2$. We define the active-sterile neutrino mixing angle as [34]

$$\theta_I^2 = \sum_{\sigma=e,\mu,\tau} \theta_{\sigma I}^2. \quad (42)$$

V. NUMERICAL RESULTS

The neutrino oscillation experimental data [5] and the lightest CP -even Higgs h^0 with a mass $m_{h^0} \simeq 125$ GeV [35] constrain relevant parameter space strongly. In numerical analysis, we adopt the relevant parameters as default,

$$\begin{aligned} v_{N_3} &= 2 \text{ TeV}, & M_1 &= 1.2 \text{ TeV}, & M_2 &= 1.6 \text{ TeV}, & m_{BBL} &= 1.3 \text{ TeV}, \\ m_A &= 1 \text{ TeV}, & g_{BL} &= 0.6, & \mu &= -1 \text{ TeV}, & (m_{Nc}^2)_{11} &= (m_{Nc}^2)_{22} = 1.8 \text{ TeV}, \\ m_{\tilde{\nu}_{L_1}} &= 2100 \text{ GeV}, & m_{\tilde{\nu}_{L_2}} &= 2200 \text{ GeV}, & m_{\tilde{\nu}_{L_3}} &= 2300 \text{ GeV}, \\ m_{\tilde{e}_{L_1}} &= 3100 \text{ GeV}, & m_{\tilde{e}_{L_2}} &= 3200 \text{ GeV}, & m_{\tilde{e}_{L_3}} &= 3300 \text{ GeV} \end{aligned} \quad (43)$$

to reduce the number of free parameters in the model considered here.

As mentioned above, the masses of two light sterile neutrinos mainly originate from one-loop radiative corrections. The corrections to the sterile neutrino masses depend on two heavy Majorana fermion masses m_{N_α} , the orthogonal matrix U_N and $U(1)_{B-L}$ gauge boson mass $m_{Z_{BL}}$ from Eq. (29). The mass $m_{Z_{BL}}$ depends on the VEVs v_{N_i} of right-handed sneutrinos. From Eqs. (13) and (14), both m_{N_α} and U_N are determined by v_{N_i} and m_{BL} which is the $U(1)_{B-L}$ gaugino mass in soft breaking terms. At the same time, these parameters affect the active neutrino masses from Eq. (34). In this section, we analyze the numerical results for the mixing angles and mass squared differences of active neutrinos varying with v_{N_2} , m_{BL} , and $\tan\beta$, assuming neutrino mass spectrum with normal ordering (NO) and inverted ordering (IO). Meanwhile, we discuss the numerical results of two sterile neutrino masses and the active-sterile neutrino mixing angles varying with these parameters.

A. NO spectrum

In order to fit the experimental data on active neutrino mass squared differences and mixing angles in this scenario, we choose the VEVs of left-handed sneutrinos and the Yukawa couplings of right-handed neutrinos, respectively, as

$$\begin{aligned}
v_{L_1} &= 1.547 \times 10^{-4} \text{ GeV}, & Y_1 &= 9.982 \times 10^{-7}, \\
v_{L_2} &= 3.220 \times 10^{-4} \text{ GeV}, & Y_2 &= 2.440 \times 10^{-6}, \\
v_{L_3} &= 1.256 \times 10^{-4} \text{ GeV}, & Y_3 &= 1.468 \times 10^{-6}.
\end{aligned} \tag{44}$$

Correspondingly the theoretical predictions on active neutrino mixing angles, mass squared differences, the sum of the active neutrino masses, two sterile neutrino masses m_{r_1} , m_{r_2} , and the active-sterile neutrino mixing angles θ_1^2 , θ_2^2 are derived as

$$\begin{aligned}
\sin^2 \theta_{12} &= 0.3072, & \sin^2 \theta_{23} &= 0.4370, & \sin^2 \theta_{13} &= 0.0234, \\
\Delta m_A^2 &= 2.430 \times 10^{-3} \text{ eV}^2, & \Delta m_\odot^2 &= 7.532 \times 10^{-5} \text{ eV}^2, & \sum_i m_{\nu_i} &= 5.798 \times 10^{-2} \text{ eV}, \\
m_{r_1} &= 7.13 \text{ KeV}, & m_{r_2} &= 12.88 \text{ KeV}, \\
\theta_1^2 &= 2.58 \times 10^{-11}, & \theta_2^2 &= 1.17 \times 10^{-10},
\end{aligned} \tag{45}$$

when $v_{N_1} = 3 \text{ GeV}$, $v_{N_2} = 7.7 \text{ GeV}$, $m_{BL} = 1.08 \text{ TeV}$, and $\tan \beta = 20$.

Assuming neutrino mass spectrum with NO and taking $v_{N_1} = 3 \text{ GeV}$, $m_{BL} = 1.08 \text{ TeV}$, and $\tan \beta = 20$, we depict the active neutrino mixing angles varying with the VEV v_{N_2} of right-handed sneutrinos in Fig. 1(a), where the solid line denotes $\sin^2 \theta_{23}$ versus v_{N_2} , the dashed line denotes $\sin^2 \theta_{12}$ versus v_{N_2} , and the dotted line denotes $\sin^2 \theta_{13}$ versus v_{N_2} . With the increasing of v_{N_2} , theoretical predictions of these mixing angles vary gently. In this region of v_{N_2} , the three mixing angles satisfy the experiment bounds simultaneously [5]. Using the same choice on parameter space, we draw the mass squared differences of active neutrinos varying with v_{N_2} in Fig. 1(b), where the solid line denotes Δm_A^2 versus v_{N_2} , and the dashed line denotes Δm_\odot^2 versus v_{N_2} . With the increasing of v_{N_2} , Δm_A^2 and Δm_\odot^2 decreases slowly. The effective mass matrix for active neutrinos depends on v_{N_2} through the term $\zeta_i \zeta_j / \Lambda_\zeta \simeq (2\tilde{\mu}^4 v_u^2 m_{BL}) / (\Lambda_{\tilde{m}^4} v_N^2)$, and v_{N_2} has relatively small influence on v_N ($v_{N_2} \ll v_N$).

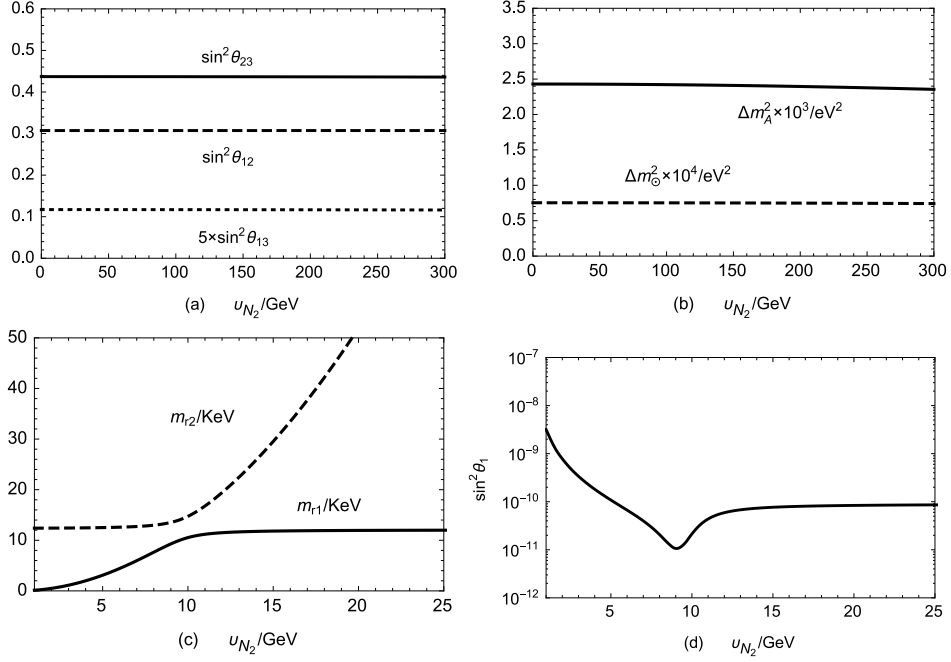


FIG. 1: Assuming neutrino mass spectrum with NO, we plot the mixing angles, mass squared differences of active neutrinos, two sterile neutrino masses, and active-sterile neutrino mixing angle versus the VEV v_{N_2} of right-handed sneutrinos, where (a) the solid line stands for $\sin^2 \theta_{23}$ versus v_{N_2} , the dashed line for stands $\sin^2 \theta_{12}$ versus v_{N_2} , and the dotted line stands for $\sin^2 \theta_{13}$ versus v_{N_2} , (b) the solid line stands for Δm_A^2 versus v_{N_2} and the dashed line stands for Δm_\odot^2 versus v_{N_2} , (c) the solid line stands for m_{r1} versus v_{N_2} and the dashed line stands for m_{r2} versus v_{N_2} , and (d) the solid line stands for $\sin^2 \theta_1$ of active-sterile neutrino mixing angle versus v_{N_2} .

Additionally, we study the two sterile neutrino masses m_{r1} , m_{r2} varying with v_{N_2} in Fig. 1(c), where the solid line denotes m_{r1} versus v_{N_2} , and the dashed line denotes m_{r2} versus v_{N_2} . It shows that two sterile neutrinos obtain KeV scale masses. When $v_{N_2} \leq 10$ GeV, m_{r1} increases steeply with the increasing of v_{N_2} , and m_{r2} changes mildly with v_{N_2} . However, when $v_{N_2} \geq 10$ GeV, the dependence of m_{r1} on v_{N_2} is not obvious, and m_{r2} increases quickly with the increasing of v_{N_2} . This is because the two sterile neutrinos obtain masses from the one-loop corrections. The corrections depend on U_N , m_{N_α} , and $m_{Z_{BL}}^2$, which are all related to v_{N_2} . Under the same choice on parameter space, the numerical result of the active-heavier sterile neutrino mixing angle $\sin^2 \theta_2$ changes gently about 10^{-10} or 10^{-11} . We only study the

active-lighter sterile neutrino mixing angle $\sin^2 \theta_1$ varying with v_{N_2} in Fig. 1(d). Considering the restrictions of X-ray line searches on the mixing angle, the applicable range of v_{N_2} is about from 5 to 12 GeV [14]. When $v_{N_2} = 7.7$ GeV, the sterile neutrino mass m_{r1} is about 7.13 KeV with the mixing angle $\sin^2 \theta_1 \sim 10^{-11}$ which can explain the observed X-ray line at 3.5 KeV [16, 17]. So, the lighter sterile neutrino can be a dark matter candidate.

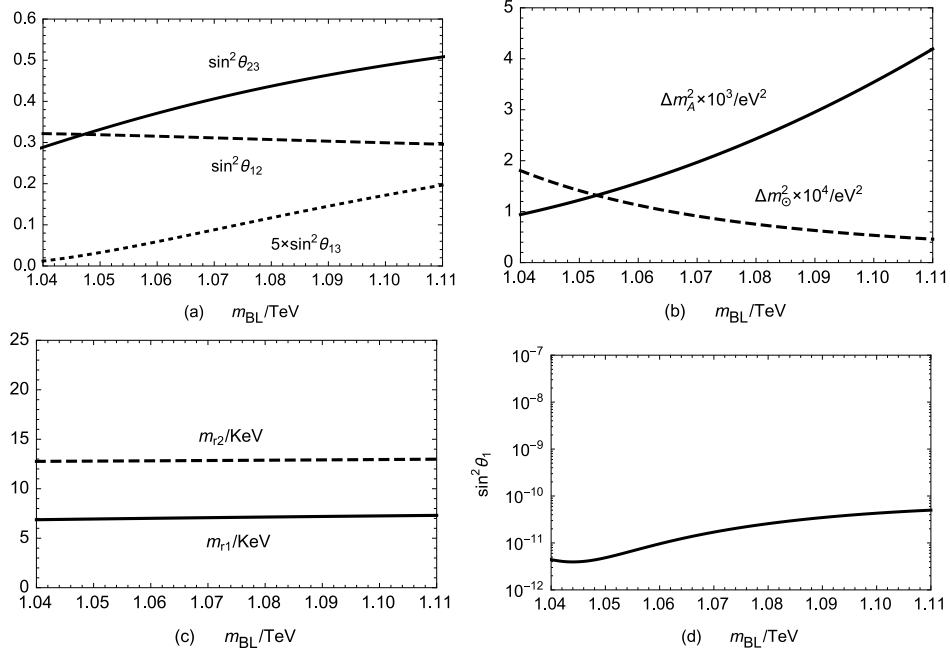


FIG. 2: Assuming neutrino mass spectrum with NO, we plot the mixing angles, mass squared differences of active neutrinos, two sterile neutrino masses and active-sterile neutrino mixing angle versus $U(1)_{B-L}$ gaugino mass m_{BL} , where (a) the solid line stands for $\sin^2 \theta_{23}$ versus m_{BL} , the dashed line stands for $\sin^2 \theta_{12}$ versus m_{BL} , and the dotted line stands for $\sin^2 \theta_{13}$ versus m_{BL} , (b) the solid line stands for Δm_A^2 versus m_{BL} and the dashed line stands for Δm_{\odot}^2 versus m_{BL} , (c) the solid line stands for m_{r1} versus m_{BL} and the dashed line stands for m_{r2} versus m_{BL} , and (d) the solid line stands for $\sin^2 \theta_1$ versus m_{BL} .

In this model, the $U(1)_{B-L}$ gaugino mass m_{BL} also affects the final numerical results of the neutrino sector. Taking $\tan \beta = 20$ and $v_{N_1} = 3$ GeV, $v_{N_2} = 7.7$ GeV; we plot the active neutrino mixing angles varying with m_{BL} in Fig. 2(a), where the solid line denotes $\sin^2 \theta_{23}$ versus v_{N_2} , the dashed line denotes $\sin^2 \theta_{12}$ versus v_{N_2} , and the dotted

line denotes $\sin^2 \theta_{13}$ versus v_{N_2} . With the increasing of m_{BL} , the theoretical prediction on the mixing angle $\sin^2 \theta_{12}$ depends on m_{BL} mildly, and the mixing angles $\sin^2 \theta_{23}$, $\sin^2 \theta_{13}$ increase steeply. Using the same choice on parameter space, we plot the mass squared differences of active neutrinos varying with m_{BL} in Fig. 2(b), where the solid line denotes Δm_A^2 versus v_{N_2} , and the dashed line denotes Δm_\odot^2 versus v_{N_2} . It shows that Δm_A^2 raises steeply with the increasing of m_{BL} , and Δm_\odot^2 diminishes quickly with the increasing of m_{BL} . The effective mass matrix for active neutrinos depends on m_{BL} through the term $\zeta_i \zeta_j / \Lambda_\zeta \simeq (2\tilde{\mu}^4 v_u^2 m_{BL}) / (\Lambda_{\tilde{m}^4} v_N^2)$; therefore, the numerical evaluations on $\sin^2 \theta_{23}$, $\sin^2 \theta_{13}$, Δm_A^2 and Δm_\odot^2 depend on m_{BL} strongly. From those numerical results on these parameter spaces, we find that the updated experiment data require $m_{BL} \sim 1.08$ TeV. Additionally we study the masses of two sterile neutrinos varying with m_{BL} in Fig. 2(c). The numerical results indicate that both m_{r1} and m_{r2} depend on m_{BL} mildly. The active-sterile neutrino mixing angle $\sin^2 \theta_2$ changes gently about 10^{-10} with the increasing of m_{BL} . We study the active-sterile neutrino mixing angle $\sin^2 \theta_1$ varying with v_{N_2} in Fig. 2(d). With increasing of m_{BL} , the mixing angle $\sin^2 \theta_1$ increases quickly.

Taking $m_{BL} = 1.08$ TeV, $v_{N_1} = 3$ GeV, and $v_{N_2} = 7.7$ GeV, we draw the active neutrino mixing angles varying with $\tan \beta$ in Fig. 3(a), where the solid line denotes Δm_A^2 versus v_{N_2} , and the dashed line denotes Δm_\odot^2 versus v_{N_2} . With the increasing of $\tan \beta$, theoretical predictions on the mixing angle $\sin^2 \theta_{12}$ varies gently, and the mixing angles $\sin^2 \theta_{23}$, and $\sin^2 \theta_{13}$ decrease slowly. Using the same choice on parameter space, we draw the mass squared differences of active neutrinos varying with $\tan \beta$ in Fig. 3(b), where the solid line denotes Δm_A^2 versus v_{N_2} , and the dashed line denotes Δm_\odot^2 versus v_{N_2} . It shows that Δm_\odot^2 varies mildly and Δm_A^2 decreases steeply with the increasing of $\tan \beta$. Additionally, we study the masses of two sterile neutrinos versus $\tan \beta$ in Fig. 3(c); the numerical result implies that two sterile neutrino masses depend on $\tan \beta$ gently. This is because two sterile neutrinos obtain masses mainly from the radiative corrections, and from Eq. (29) the corrections on masses of two sterile neutrinos are almost not dependent on $\tan \beta$. For the same reason, the active-sterile neutrino mixing angle has barely changed with $\tan \beta$. The numerical result of $\sin^2 \theta_2$ is about 10^{-10} . The numerical result of $\sin^2 \theta_1$ is about 10^{-11} in Fig. 3(d).

Assuming neutrino mass spectrum with normal ordering, two sterile neutrinos obtain

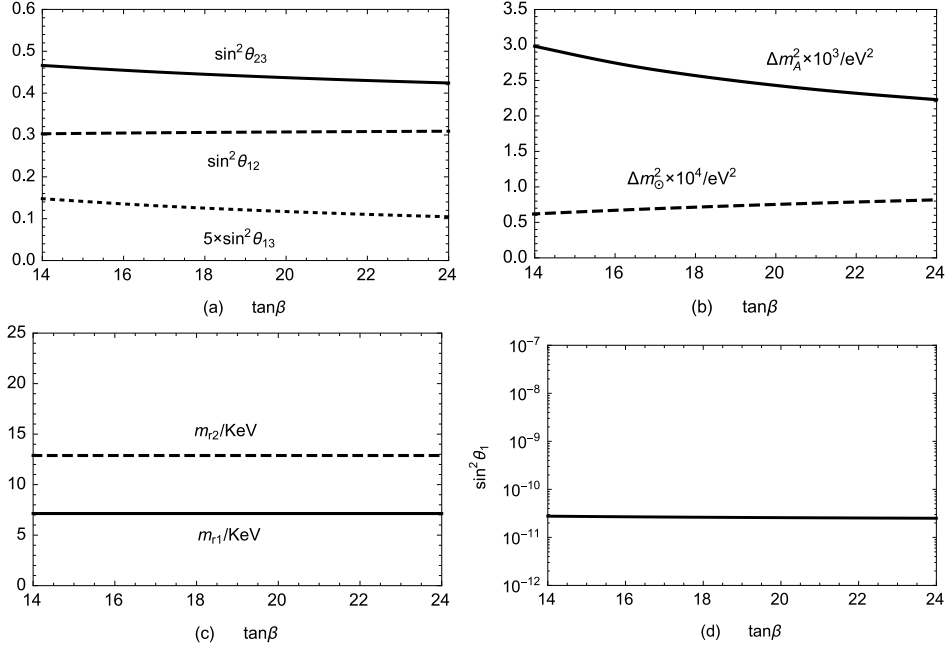


FIG. 3: Assuming neutrino mass spectrum with NO, we plot the mixing angles, mass squared differences of active neutrinos, two sterile neutrino masses and active-sterile neutrino mixing angle versus $\tan\beta$, where (a) the solid line stands for $\sin^2\theta_{23}$ versus $\tan\beta$, the dashed line stands for $\sin^2\theta_{12}$ versus $\tan\beta$, and the dotted line stands for $\sin^2\theta_{13}$ versus $\tan\beta$, (b) the solid line stands for Δm_A^2 versus $\tan\beta$ and the dashed line stands for Δm_\odot^2 versus $\tan\beta$, (c) the solid line stands for m_{r1} versus $\tan\beta$ and the dashed line stands for m_{r2} versus $\tan\beta$, and (d) the solid line stands for $\sin^2\theta_1$ versus $\tan\beta$.

KeV scale masses. Both KeV sterile neutrinos were produced in the early Universe via oscillations. The lighter sterile neutrino forms dark matter, but the oscillation mechanism cannot produce enough of these neutrinos to act as all dark matter for given m_{r1} and $\sin^2\theta_1$ [37, 38]. The heavier sterile neutrino can decay into the lighter one to enrich the production of the sterile neutrino DM.

B. IO spectrum

With the active neutrino mass spectrum being IO spectrum, we choose the VEVs of left-handed sneutrinos and the Yukawa couplings of sterile neutrinos, respectively, as

$$\begin{aligned}
v_{L_1} &= 1.899 \times 10^{-4} \text{ GeV}, & Y_1 &= 4.989 \times 10^{-7}, \\
v_{L_2} &= 4.208 \times 10^{-4} \text{ GeV}, & Y_2 &= 2.896 \times 10^{-6}, \\
v_{L_3} &= 3.434 \times 10^{-4} \text{ GeV}, & Y_3 &= 2.551 \times 10^{-6}.
\end{aligned} \tag{46}$$

Correspondingly the theoretical predictions on active neutrino mixing angles, mass squared differences, the sum of the active neutrino masses, two sterile neutrino masses m_{r1} , m_{r2} , and the active-sterile neutrino mixing angles θ_1^2 , θ_2^2 are derived as

$$\begin{aligned}
\sin^2 \theta_{12} &= 0.3077, & \sin^2 \theta_{23} &= 0.4556, & \sin^2 \theta_{13} &= 0.0243, \\
\Delta m_A^2 &= 2.381 \times 10^{-3} \text{ eV}^2, & \Delta m_\odot^2 &= 7.627 \times 10^{-5} \text{ eV}^2, & \sum_i m_{\nu_i} &= 9.682 \times 10^{-2} \text{ eV}, \\
m_{r1} &= 7.13 \text{ KeV}, & m_{r2} &= 12.88 \text{ KeV}, \\
\theta_1^2 &= 2.84 \times 10^{-11}, & \theta_2^2 &= 3.27 \times 10^{-10},
\end{aligned} \tag{47}$$

when $v_{N_1} = 3 \text{ GeV}$, $v_{N_2} = 7.7 \text{ GeV}$, $m_{BL} = 1.08 \text{ TeV}$, and $\tan \beta = 20$.

When the neutrino mass spectrum is IO, the manners of parameters v_{N_2} , m_{BL} , and $\tan \beta$ affecting the numerical results on the neutrino sector may differ from that of the neutrino mass spectrum with NO. Assuming neutrino mass spectrum with IO and taking $v_{N_1} = 3 \text{ GeV}$, $m_{BL} = 1.08 \text{ TeV}$, and $\tan \beta = 20$, we depict the active neutrino mixing angles varying with v_{N_2} in Fig. 4(a), where the solid line denotes $\sin^2 \theta_{23}$ versus v_{N_2} , the dashed line denotes $\sin^2 \theta_{12}$ versus v_{N_2} , and the dotted line denotes $\sin^2 \theta_{13}$ versus v_{N_2} . Obviously, theoretical predictions on those mixing angles vary slowly with the increasing of v_{N_2} . Adopting the same choice on parameter space, we draw the mass squared differences of active neutrinos varying with v_{N_2} in Fig. 4(b), where the solid line denotes Δm_A^2 versus v_{N_2} , and the dashed line denotes Δm_\odot^2 versus v_{N_2} . It shows that Δm_A^2 decreases gently with the increasing of v_{N_2} , but Δm_\odot^2 decreases steeply. Taking into account the neutrino experiment bounds, the appropriate region of v_{N_2} is $v_{N_2} \leq 60 \text{ GeV}$. In addition, we study the masses of two sterile neutrinos varying with v_{N_2} in Fig. 4(c), where the solid line denotes m_{r1} versus

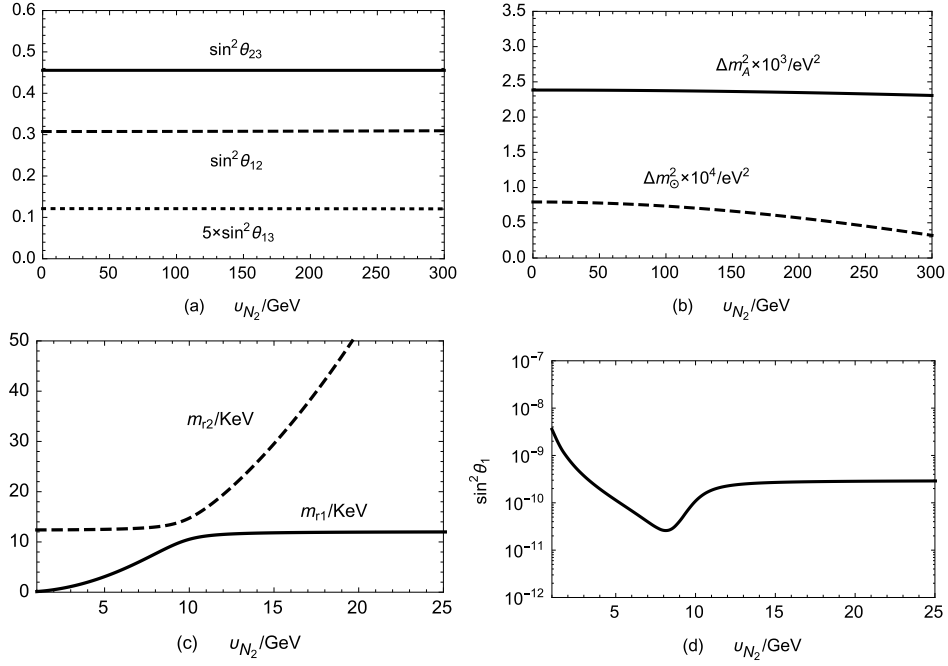


FIG. 4: Assuming neutrino mass spectrum with IO, we plot the mixing angles, mass squared differences of active neutrinos, two sterile neutrino masses and active-sterile neutrino mixing angle versus the VEV v_{N_2} of right-handed sneutrinos, where (a) the solid line stands for $\sin^2 \theta_{23}$ versus v_{N_2} , the dashed line stands for $\sin^2 \theta_{12}$ versus v_{N_2} , and the dotted line stands for $\sin^2 \theta_{13}$ versus v_{N_2} , (b) the solid line stands for Δm_A^2 versus v_{N_2} and the dashed line stands for Δm_\odot^2 versus v_{N_2} , (c) the solid line stands for m_{r1} versus v_{N_2} and the dashed line stands for m_{r2} versus v_{N_2} , and (d) the solid line stands for $\sin^2 \theta_1$ of active-sterile neutrino mixing angle versus v_{N_2} .

v_{N_2} , and the dashed line denotes m_{r2} versus v_{N_2} . It shows that two sterile neutrinos masses have almost the same changing trend as the NO spectrum. Because two sterile neutrinos obtain relatively large masses than active neutrinos, they are almost irrelevant to the active neutrino mass spectrum. Under the same choice on parameter space, the numerical result of the active-heavier sterile neutrino mixing angle $\sin^2 \theta_2$ changes gently about 10^{-10} . We only study the active-lighter sterile neutrino mixing angle $\sin^2 \theta_1$ versus v_{N_2} in Fig. 4(d). It shows that the mixing angle $\sin^2 \theta_1$ depends on v_{N_2} strongly. Considering the restrictions of X-ray line searches on the mixing angle, the applicable range of v_{N_2} is about from 5 to 10 GeV [14]. When $v_{N_2} = 7.7$ GeV, the sterile neutrino mass m_{r1} is about 7.13 KeV with

the mixing angle $\sin^2 \theta_1 \sim 10^{-11}$ which can explain the observed X-ray line at 3.5 KeV [16, 17]. Therefore, the lighter sterile neutrino can be a dark matter candidate.

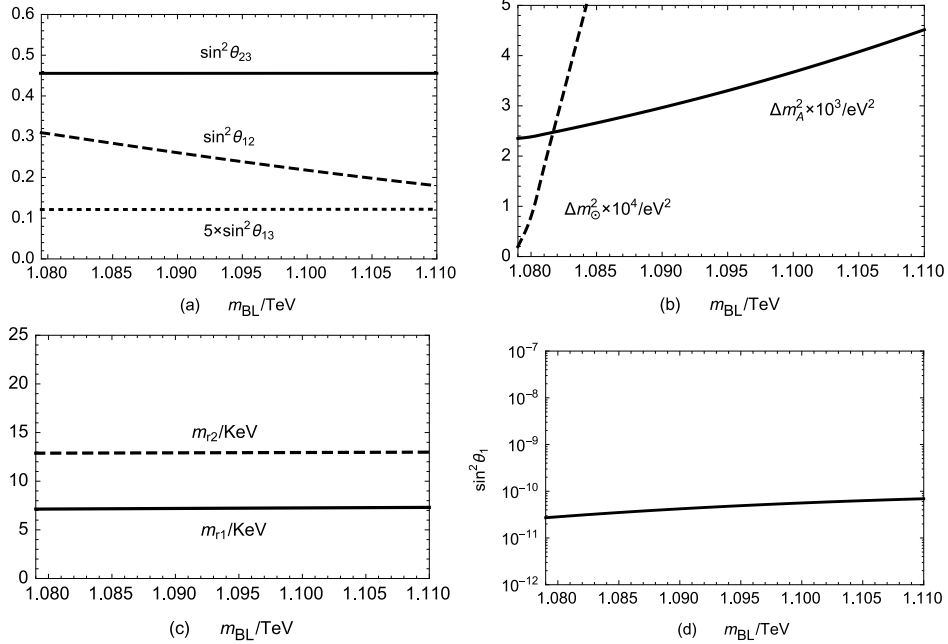


FIG. 5: Assuming neutrino mass spectrum with IO, we plot the mixing angles, mass squared differences of active neutrinos, two sterile neutrino masses and active-sterile neutrino mixing angle versus $U(1)_{B-L}$ gaugino mass m_{BL} , where (a) the solid line stands for $\sin^2 \theta_{23}$ versus m_{BL} , the dashed line stands for $\sin^2 \theta_{12}$ versus m_{BL} , and the dotted line stands for $\sin^2 \theta_{13}$ versus m_{BL} , (b) the solid line stands for Δm_A^2 versus m_{BL} and the dashed line stands for Δm_C^2 versus m_{BL} , (c) the solid line stands for m_{r1} versus m_{BL} and the dashed line stands for m_{r2} versus m_{BL} , and (d) the solid line stands for $\sin^2 \theta_1$ versus m_{BL} .

Taking $\tan \beta = 20$, $v_{N_1} = 3$ GeV, and $v_{N_2} = 7.7$ GeV, we plot the active neutrino mixing angles varying with m_{BL} in Fig. 5(a), where the solid line denotes $\sin^2 \theta_{23}$ versus v_{N_2} , the dashed line denotes $\sin^2 \theta_{12}$ versus v_{N_2} , and the dotted line denotes $\sin^2 \theta_{13}$ versus v_{N_2} . With the increasing of m_{BL} , the theoretical predictions on the mixing angles of active neutrinos $\sin^2 \theta_{23}$ and $\sin^2 \theta_{13}$ depend on m_{BL} mildly, and the mixing angle $\sin^2 \theta_{12}$ decreases steeply. Adopting the same choice on parameter space, we plot the mass squared differences of active neutrinos varying with m_{BL} in Fig. 5(b), where the solid line denotes Δm_A^2 versus m_{BL} and

the dashed line denotes Δm_{\odot}^2 versus m_{BL} . It shows that the mass squared differences of active neutrinos Δm_A^2 and Δm_{\odot}^2 increase steeply with the increasing of m_{BL} . From those numerical results, we find that the updated experimental data require $m_{BL} \sim 1.08$ TeV. In addition, we study the masses of two sterile neutrinos varying with ν_{N_2} in Fig. 5(c), where the solid line denotes m_{r_1} versus m_{BL} and the dashed line denotes m_{r_2} versus m_{BL} . It shows that the two sterile neutrino masses have the same trend of variability with the NO spectrum. Under the same choice on parameter space, the numerical result of the active-heavier sterile neutrino mixing angle $\sin^2 \theta_2$ changes gently about 10^{-10} . We only study the active-sterile neutrino mixing angle $\sin^2 \theta_1$ versus m_{BL} in Fig. 5(d). With increasing of m_{BL} , the active-sterile neutrino mixing angle $\sin^2 \theta_1$ increases gently.

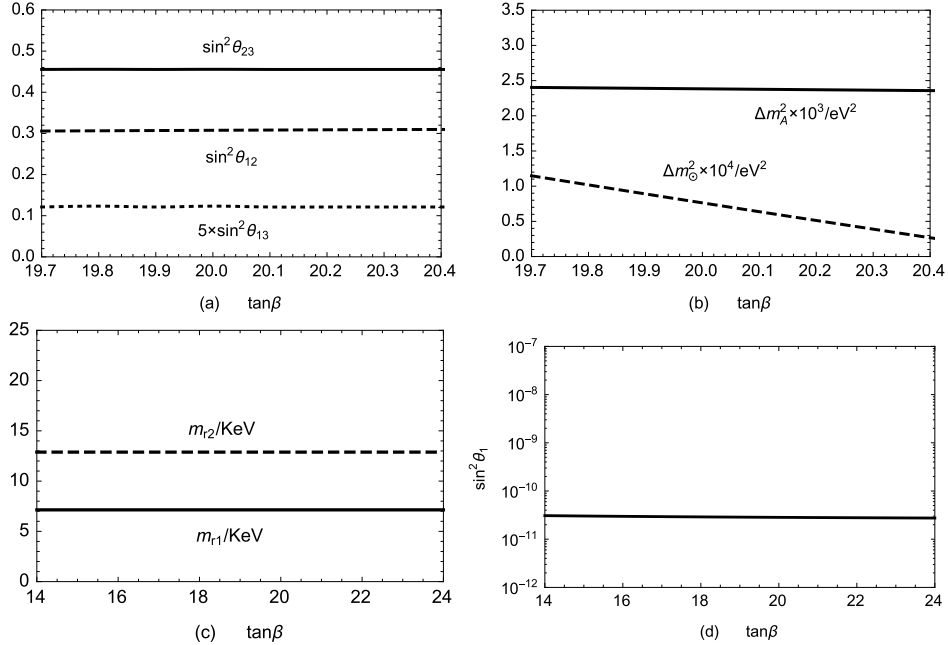


FIG. 6: Assuming neutrino mass spectrum with IO, we plot the mixing angles, mass squared differences of active neutrinos, two sterile neutrino masses and active-sterile neutrino mixing angle versus $\tan\beta$, where (a) the solid line stands for $\sin^2 \theta_{23}$ versus $\tan\beta$, the dashed line stands for $\sin^2 \theta_{12}$ versus $\tan\beta$, and the dotted line stands for $\sin^2 \theta_{13}$ versus $\tan\beta$, (b) the solid line stands for Δm_A^2 versus $\tan\beta$ and the dashed line stands for Δm_{\odot}^2 versus $\tan\beta$, (c) the solid line stands for m_{r_1} versus $\tan\beta$ and the dashed line stands for m_{r_2} versus $\tan\beta$, and (d) the solid line stands for $\sin^2 \theta_1$ versus $\tan\beta$.

Taking $m_{BL} = 1.08$ TeV, $v_{N_1} = 3$ GeV, and $v_{N_2} = 7.7$ GeV, we draw the neutrino mixing angles varying with $\tan \beta$ in Fig. 6(a). With the increasing of $\tan \beta$, theoretical predictions on those mixing angles vary gently. Adopting the same choice on parameter space, we draw the mass squared differences of active neutrinos varying with $\tan \beta$ in Fig. 6(b). It shows that Δm_A^2 (solid line) changes gently with the increasing of $\tan \beta$; however, Δm_\odot^2 (dashed line) decreases rapidly with the increasing of $\tan \beta$. In addition, we study the masses of two sterile neutrinos versus $\tan \beta$ in Fig. 6(c). It shows that the masses of two sterile neutrinos depend on $\tan \beta$ gently. The active-sterile neutrino mixing angles have barely changed with $\tan \beta$. The numerical result of $\sin^2 \theta_2$ is about 10^{-10} . The numerical result of $\sin^2 \theta_1$ is about 10^{-11} in Fig. 6(d).

Assuming the neutrino mass spectrum with inverted ordering, two sterile neutrinos obtain KeV scale masses. The lighter sterile neutrino forms dark matter, and the heavier sterile neutrino can decay into the lighter one to enrich the production of the sterile neutrino DM.

VI. SUMMARY

We investigate the origin of neutrino masses in the MSSM with local $U(1)_{B-L}$ symmetry. In this model sneutrinos all obtain nonzero VEVs. We constrain the relevant parameter space by the neutrino oscillation experimental data and the mass of the lightest CP -even Higgs. At tree level, three left-handed neutrinos and two sterile neutrinos obtain masses through the seesaw mechanism, but the masses of two sterile neutrinos are very tiny. The one-loop radiation corrections to the mass matrix of neutralino-neutrino are also studied. Both NO spectrum and IO spectrum are studied. The active neutrino mass squared differences and mixing angles can account for the experimental data on neutrino oscillations. Because the one-loop radiative corrections to the left-handed neutrinos are suppressed by the tiny Yukawa couplings and the small nonzero VEVs of left-handed sneutrinos, the corrections to the active neutrinos are very small. The active neutrinos obtain mass mainly from tree level. When one-loop corrections are included, the numerical results show that there is parameter space to give two sterile neutrinos with KeV masses and the small active-sterile neutrino mixing angle. When $v_{N_2} = 7.7$ GeV, $m_{BL} = 1.08$ TeV, and $\tan \beta = 20$, the mass

of the heavier sterile neutrino m_{r2} is about 12.88 KeV, the mixing angle $\sin^2 \theta_2$ is about 10^{-10} , the mass of lighter sterile neutrino m_{r1} is about 7.1 KeV, and the mixing angle $\sin^2 \theta_1$ is about 10^{-11} . The lighter sterile neutrino can account for the observed X-ray line at 3.5 KeV [16, 17]. Therefore, the lighter sterile neutrino can be a dark matter candidate. However the oscillation mechanism does not produce enough of these neutrinos to act as all dark matter [36, 37]. Nonresonant production contributes to the dark matter abundance $\Omega_s h^2 \approx 0.3(\frac{\sin^2 2\theta}{10^{-10}})(\frac{m_r}{100\text{keV}})^2$ [37]. Only 1% of dark matter is produced for the lightest sterile neutrino. In this model, the heavier sterile neutrino can decay into the lighter one to enrich the production of the sterile neutrino DM. However, this still does not produce enough dark matter and it may require other mechanisms (Shi-Fuller mechanism [38]) in the early Universe [14].

Acknowledgments

The work has been supported by the National Natural Science Foundation of China (NNSFC) with Grants No. 11275036, No. 11535002, No. 11647120, and No. 11705045, the Natural Science Foundation of Hebei province with Grants No.A2016201010, and A2016201069, the Natural Science Foundation of Hebei University with Grants No. 2011JQ05, and No. 2012-242, and the Hebei Key Lab of Optic-Electronic Information and Materials.

Appendix A: The effective mass matrices for right-handed sneutrinos

Considering the last minimization condition in Eq. (8), the most general matrix is

$$m_{\tilde{N}^c}^2 = \begin{pmatrix} \frac{\xi_{\tilde{N}_1^c}^2 - m_{ZBL}^2/2}{-\xi_{\tilde{N}_1^c}^2 v_{N_1} - \xi_{\tilde{N}_2^c}^2 v_{N_2} + \xi_{\tilde{N}_3^c}^2 v_{N_3}} & \frac{-\xi_{\tilde{N}_1^c}^2 v_{N_1} - \xi_{\tilde{N}_2^c}^2 v_{N_2} + \xi_{\tilde{N}_3^c}^2 v_{N_3}}{2v_{N_1} v_{N_2}} & \frac{-\xi_{\tilde{N}_1^c}^2 v_{N_1} + \xi_{\tilde{N}_2^c}^2 v_{N_2} - \xi_{\tilde{N}_3^c}^2 v_{N_3}}{2v_{N_1} v_{N_3}} \\ \frac{-\xi_{\tilde{N}_1^c}^2 v_{N_1} - \xi_{\tilde{N}_2^c}^2 v_{N_2} + \xi_{\tilde{N}_3^c}^2 v_{N_3}}{2v_{N_1} v_{N_2}} & \xi_{\tilde{N}_2^c}^2 - m_{ZBL}^2/2 & \frac{\xi_{\tilde{N}_1^c}^2 v_{N_1} - \xi_{\tilde{N}_2^c}^2 v_{N_2} - \xi_{\tilde{N}_3^c}^2 v_{N_3}}{2v_{N_2} v_{N_3}} \\ \frac{-\xi_{\tilde{N}_1^c}^2 v_{N_1} + \xi_{\tilde{N}_2^c}^2 v_{N_2} - \xi_{\tilde{N}_3^c}^2 v_{N_3}}{2v_{N_1} v_{N_3}} & \frac{\xi_{\tilde{N}_1^c}^2 v_{N_1} - \xi_{\tilde{N}_2^c}^2 v_{N_2} - \xi_{\tilde{N}_3^c}^2 v_{N_3}}{2v_{N_2} v_{N_3}} & \xi_{\tilde{N}_3^c}^2 - m_{ZBL}^2/2 \end{pmatrix}, \quad (\text{A1})$$

with $\xi_{\tilde{N}_1^c}^2 = (m_{\tilde{N}^c}^2)_{11} + m_{ZBL}^2/2$, $\xi_{\tilde{N}_2^c}^2 = (m_{\tilde{N}^c}^2)_{22} + m_{ZBL}^2/2$, and $\xi_{\tilde{N}_3^c}^2 = (m_{\tilde{N}^c}^2)_{33} + m_{ZBL}^2/2$. There are three parameters in matrix $m_{\tilde{N}^c}^2$. We make an approximation of this matrix to

reduce the number of free parameters. A possible solution is that v_{N_1} and v_{N_2} are small and v_{N_3} is large for large v_N ($v_N^2 = \sum_{\alpha=1}^3 v_{N_\alpha}^2$). In this case, we can obtain $(m_{\tilde{N}^c}^2)_{33} \simeq -m_{Z_{BL}}^2/2$ from the last minimization condition in Eq. (8). Compared to $(m_{\tilde{N}^c}^2)_{33} = \xi_{\tilde{N}_3^c}^2 - m_{Z_{BL}}^2/2$ in Eq. (B1), $\xi_{\tilde{N}_3^c}^2$ should be small. If we select the appropriate parameters $\xi_{\tilde{N}_{1,2}^c}^2$ and choose $\xi_{\tilde{N}_3^c}^2 = \frac{\xi_{\tilde{N}_1^c}^2 v_{N_1} + \xi_{\tilde{N}_2^c}^2 v_{N_2}}{v_{N_3}}$, $\xi_{\tilde{N}_3^c}^2$ should be small considering small $v_{N_{1,2}}$ and large v_{N_3} . The number of matrix parameters is reduced to two. Then, we can have Eq.(9).

Using the minimization conditions, we derive the 3×3 mass squared matrix for neutral CP -odd scalars $P_{\tilde{N}^c}^0$ at tree level

$$(M_{\tilde{N}^c}^2)^{odd}_{IJ} = (m_{\tilde{N}^c}^2)_{IJ} + \frac{m_{Z_{BL}}^2}{2} \delta_{IJ}, \quad (\text{A2})$$

with $I, J = 1, 2, 3$ denoting the index of generation. Correspondingly the orthogonal 3×3 matrix from interaction eigenstates to mass eigenstates is written as $U_{\tilde{N}^c}$, and three masses of the CP -odd scalars are

$$m_{P_{\tilde{N}_1}^0}^2 = 0, \quad m_{P_{\tilde{N}_2}^0}^2 = \frac{\omega_A - \omega_B}{2v_{N_3}^2}, \quad m_{P_{\tilde{N}_3}^0}^2 = \frac{\omega_A + \omega_B}{2v_{N_3}^2}. \quad (\text{A3})$$

and the concrete expressions for $\omega_{A,B}$ are

$$\begin{aligned} \omega_A &= \xi_{\tilde{N}_1^c}^2 (v_N^2 - v_{N_2}^2) + \xi_{\tilde{N}_2^c}^2 (v_N^2 - v_{N_1}^2), \\ \omega_B &= \omega_A^2 - 4\xi_{\tilde{N}_1^c}^2 \xi_{\tilde{N}_2^c}^2 v_N^2 v_{N_3}^2. \end{aligned} \quad (\text{A4})$$

Additionally the 3×3 mass squared matrix for neutral CP -even scalars $\tilde{\nu}_{R_I}$ is

$$(M_{\tilde{N}^c}^2)^{even}_{IJ} = (m_{\tilde{N}^c}^2)_{IJ} + \frac{m_{Z_{BL}}^2}{2} \delta_{IJ} + g_{BL}^2 v_{N_I} v_{N_J}. \quad (\text{A5})$$

Correspondingly the orthogonal 3×3 matrix is written as $U_{\tilde{N}^c}$, and three masses of the CP -even scalars are

$$m_{H_{\tilde{N}_1}^0}^2 = m_{Z_{BL}}^2, \quad m_{H_{\tilde{N}_2}^0}^2 = \frac{\omega_A - \omega_B}{2v_{N_3}^2}, \quad m_{H_{\tilde{N}_3}^0}^2 = \frac{\omega_A + \omega_B}{2v_{N_3}^2}. \quad (\text{A6})$$

Appendix B: The effective mass matrix for five light neutrinos at tree level

The effective mass matrix for five light neutrinos at tree level is

$$m_\nu^{eff} \simeq \begin{pmatrix} [M_\nu^{LL}]_{3 \times 3} & [M_\nu^{LR}]_{3 \times 2} \\ [M_\nu^{LR,T}]_{2 \times 3} & [M_\nu^{RR}]_{2 \times 2} \end{pmatrix}, \quad (\text{B1})$$

where

$$\begin{aligned}
(M_\nu^{LL})_{ij} &= \frac{v_{L_i} v_{L_j}}{\Lambda_\nu} + \frac{v_{L_i} \zeta_j + v_{L_j} \zeta_i}{\Lambda_{\nu\zeta}} + \frac{\zeta_i \zeta_j}{\Lambda_\zeta}, \\
(M_\nu^{LR})_{i1} &= \delta_{i3}, & (M_\nu^{LR})_{i2} &= \delta_{i2}, \\
(M_\nu^{RR})_{11} &= \frac{\tilde{m}(m_{BL}^2 - \Delta_{BL}^2)v_d^2}{\Lambda_{\tilde{m}^4}} \varepsilon_{13}^2, \\
(M_\nu^{RR})_{12} &= \frac{\tilde{m}(m_{BL}^2 - \Delta_{BL}^2)v_d^2}{\Lambda_{\tilde{m}^4}} \varepsilon_{12} \varepsilon_{13}, \\
(M_\nu^{RR})_{22} &= \frac{\tilde{m}(m_{BL}^2 - \Delta_{BL}^2)v_d^2}{\Lambda_{\tilde{m}^4}} \varepsilon_{12}^2,
\end{aligned} \tag{B2}$$

with

$$\begin{aligned}
\frac{1}{\Lambda_\nu} &= \frac{(m_{BL}^2 - \Delta_{BL}^2)\tilde{m}}{\Lambda_{\tilde{m}^4}} \mu^2, \\
\frac{1}{\Lambda_\zeta} &= \frac{2\tilde{\mu}^4 v_u^2 m_{BL}}{\Lambda_{\tilde{m}^4} v_N^2} + \frac{(m_{BL}^2 - \Delta_{BL}^2)\tilde{m}}{2\Lambda_{\tilde{m}^4}} v_d^2, \\
\frac{1}{\Lambda_{\nu\zeta}} &= \frac{\sqrt{2}\tilde{\mu}^4 g_{BL}^2 v_u}{\Lambda_{\tilde{m}^4}} + \frac{(m_{BL}^2 - \Delta_{BL}^2)\mu\tilde{m}}{\sqrt{2}\Lambda_{\tilde{m}^4}} v_d, \\
\Lambda_{\tilde{m}^4} &= 2(\Delta_{BL}^2 - m_{BL}^2)\tilde{\mu}^2 + (\Delta_{BL} + m_{BL})\tilde{m}v_d^2 \varepsilon_-^2 + (m_{BL} - \Delta_{BL})\tilde{m}v_d^2 \varepsilon_+^2, \\
\tilde{m} &= \frac{1}{2}(g_1^2 M_2 + g_2^2 M_1), \\
\tilde{\mu}^4 &= M_1 M_2 \mu^2 - \tilde{m} \mu v_d v_u.
\end{aligned} \tag{B3}$$

Appendix C: Radiative corrections on masses of sterile neutrinos

As $\alpha = 1, 2$ and $\beta = 3, 4$, the renormalized self-energy is formulated as

$$\begin{aligned}
\hat{\Sigma}_{\alpha\beta}^L(p^2) &= \hat{\Sigma}_{\alpha\beta}^{L(1)}(p^2) + \hat{\Sigma}_{\alpha\beta}^{L(2)}(p^2), \\
\hat{\Sigma}_{\alpha\beta}^M(p^2) &= \hat{\Sigma}_{\alpha\beta}^{M(1)}(p^2) + \hat{\Sigma}_{\alpha\beta}^{M(2)}(p^2).
\end{aligned} \tag{C1}$$

In view of $(U_N)_{41} = (U_N)_{42} = 0$, and $m_{N_{1,2}} \ll m_{N_{3,4}}$, the corrections to the mass matrix are

$$\begin{aligned}
(\Delta \mathcal{M}_N^{(0)})_{\alpha\beta} &= \frac{g_{BL}^2}{(4\pi)^2} \sum_{\delta=3}^4 \sum_{i,j}^3 m_{N_\delta} \{ \mathcal{R}((U_N)_{i\alpha} (U_N)_{4\delta} (U_N)_{j\delta} (U_N)_{4\beta}) \\
&\quad \times [\sum_{a=1}^3 (U_{\tilde{N}_E})_{ia} (U_{\tilde{N}_E})_{ja} \hat{B}_0(m_{N_\alpha}^2, m_{N_\delta}^2, m_{H_{N_a}}^2)
\end{aligned}$$

$$\begin{aligned}
& - \sum_{a=2}^3 (U_{\tilde{N}_O})_{ia} (U_{\tilde{N}_O})_{ja} \hat{B}_0(m_{N_\alpha}^2, m_{N_\delta}^2, m_{P_{N_a}}^2)] \\
& + \mathcal{R}(2(U_N)_{i\alpha} (U_N)_{i\delta}^* (U_N)_{j\delta}^* (U_N)_{j\beta}) (\hat{B}_0 - \frac{1}{2})(m_{N_\alpha}^2, m_{N_\delta}^2, m_{Z_{BL}}^2) \\
& + \mathcal{R}(2(U_N)_{i\beta} (U_N)_{i\delta}^* (U_N)_{j\delta}^* (U_N)_{j\alpha}) (\hat{B}_0 - \frac{1}{2})(m_{N_\beta}^2, m_{N_\delta}^2, m_{Z_{BL}}^2) \} \\
& - \frac{g_{BL}^2}{(4\pi)^2} m_{N_\beta} \sum_{\delta=1}^4 \sum_{i,j}^3 \mathcal{R}((U_N)_{i\beta}^* (U_N)_{i\delta}^* (U_N)_{j\delta}^* (U_N)_{j\alpha}) \\
& \quad \times (\hat{B}_1 - \frac{1}{2})(m_{N_\beta}^2, m_{N_\delta}^2, m_{Z_{BL}}^2). \tag{C2}
\end{aligned}$$

As $\alpha, \beta = 3, 4$, the result of one-loop corrections to the mass matrix is

$$\begin{aligned}
(\Delta \mathcal{M}_N^{(0)})_{\alpha\beta} &= \frac{g_{BL}^2}{(4\pi)^2} \sum_{\delta=3}^4 \sum_{i,j}^3 m_{N_\delta} \{ \mathcal{R}((U_N)_{i\alpha} (U_N)_{4\delta} (U_N)_{j\delta} (U_N)_{4\beta}) \\
& \quad \times [\sum_{a=1}^3 (U_{\tilde{N}_E})_{ia} (U_{\tilde{N}_E})_{ja} \hat{B}_0(m_{N_\alpha}^2, m_{N_\delta}^2, m_{H_{N_a}}^2) \\
& \quad - \sum_{a=2}^3 (U_{\tilde{N}_O})_{ia} (U_{\tilde{N}_O})_{ja} \hat{B}_0(m_{N_\alpha}^2, m_{N_\delta}^2, m_{P_{N_a}}^2)] \\
& \quad + \mathcal{R}(2(U_N)_{i\alpha} (U_N)_{i\delta}^* (U_N)_{j\delta}^* (U_N)_{j\beta}) (\hat{B}_0 - \frac{1}{2})(m_{N_\alpha}^2, m_{N_\delta}^2, m_{Z_{BL}}^2) + (\alpha \leftrightarrow \beta) \} \\
& - \frac{g_{BL}^2}{(4\pi)^2} \sum_{\delta=1}^4 \sum_{i,j}^3 \{ m_{N_\alpha} \mathcal{R}((U_N)_{i\alpha}^* (U_N)_{4\delta}^* (U_N)_{j\delta} (U_N)_{4\beta}) \\
& \quad \times [\sum_{a=1}^3 (U_{\tilde{N}_E})_{ia} (U_{\tilde{N}_E})_{ja} \hat{B}_1(m_{N_\alpha}^2, m_{N_\delta}^2, m_{H_{N_a}}^2) \\
& \quad + \sum_{a=1}^3 (U_{\tilde{N}_O})_{ia} (U_{\tilde{N}_O})_{ja} \hat{B}_1(m_{N_\alpha}^2, m_{N_\delta}^2, m_{P_{N_a}}^2)] \\
& \quad + \mathcal{R}((U_N)_{i\alpha}^* (U_N)_{i\delta}^* (U_N)_{j\delta}^* (U_N)_{j\beta}) (\hat{B}_1 - \frac{1}{2})(m_{N_\alpha}^2, m_{N_\delta}^2, m_{Z_{BL}}^2) \\
& \quad + (\alpha \leftrightarrow \beta) \}. \tag{C3}
\end{aligned}$$

The corrections from real and image components of right-handed sneutrinos only appear as $\beta = 3, 4$, so their contributions to the sterile neutrino masses are relatively small.

[1] S. Chatrchyan *et al.* [CMS Collaboration], Phys. Lett. B **716**, 30 (2012).

[2] G. Aad *et al.* [ATLAS Collaboration], Phys. Lett. B **716**, 1 (2012).

- [3] B. Pontecorvo, Sov. Phys. JETP **7**, 172 (1958) [Zh. Eksp. Teor. Fiz. **34**, 247 (1957)].
- [4] Z. Maki, M. Nakagawa and S. Sakata, Prog. Theor. Phys. **28**, 870 (1962).
- [5] F. Capozzi, G. L. Fogli, E. Lisi, A. Marrone, D. Montanino and A. Palazzo, Phys. Rev. D **89**, 093018 (2014).
- [6] R. Barbier *et al.*, Phys. Rept. **420**, 1 (2005).
- [7] V. Barger, P. Fileviez Perez and S. Spinner, Phys. Rev. Lett. **102**, 181802 (2009).
- [8] P. Fileviez Perez and S. Spinner, Phys. Lett. B **673**, 251 (2009).
- [9] P. Fileviez Perez and S. Spinner, Phys. Rev. D **80**, 015004 (2009).
- [10] V. Barger, P. Fileviez Perez and S. Spinner, Phys. Lett. B **696**, 509 (2011).
- [11] D. K. Ghosh, G. Senjanovic and Y. Zhang, Phys. Lett. B **698**, 420 (2011).
- [12] P. Fileviez Perez and S. Spinner, JHEP **1204**, 118 (2012).
- [13] C. H. Chang, T. F. Feng, Y. L. Yan, H. B. Zhang and S. M. Zhao, Phys. Rev. D **90**, no. 3, 035013 (2014).
- [14] M. Drewes *et al.*, JCAP **1701**, no. 01, 025 (2017). arXiv:1602.04816 [hep-ph].
- [15] S. Tremaine and J. E. Gunn, Phys. Rev. Lett. **42** (1979) 407. P. Bode, J. P. Ostriker and N. Turok, Astrophys. J. **556**, 93 (2001).
- [16] A. Boyarsky, O. Ruchayskiy, D. Iakubovskiy and J. Franse, Phys. Rev. Lett. **113**, 251301 (2014).
- [17] E. Bulbul, M. Markevitch, A. Foster, R. K. Smith, M. Loewenstein and S. W. Randall, Astrophys. J. **789**, 13 (2014).
- [18] T. Lasserre, K. Altenmueller, M. Cribier, A. Merle, S. Mertens and M. Vivier, arXiv:1609.04671 [hep-ex].
- [19] J. König, A. Merle and M. Totzauer, JCAP **1611**, no. 11, 038 (2016).
- [20] T. E. Jeltema and S. Profumo, Mon. Not. Roy. Astron. Soc. **450**, no. 2, 2143 (2015).
- [21] D. Malyshev, A. Neronov and D. Eckert, Phys. Rev. D **90**, 103506 (2014).
- [22] P. Ghosh, P. Dey, B. Mukhopadhyaya and S. Roy, JHEP **1005**, 087 (2010).
- [23] S. M. Zhao, T. F. Feng, X. X. Dong, H. B. Zhang, G. Z. Ning and T. Guo, Nucl. Phys. B **910**, 225 (2016).
- [24] T. F. Feng, Y. L. Yan, H. B. Zhang and S. M. Zhao, Phys. Rev. D **92**, no. 5, 055024 (2015).

- [25] T. F. Feng, Y. L. Yan, H. B. Zhang and S. M. Zhao, *Int. J. Mod. Phys. A* **31**, no. 16, 1650092 (2016).
- [26] T. F. Feng, J. L. Yang, H. B. Zhang, S. M. Zhao and R. F. Zhu, *Phys. Rev. D* **94**, no. 11, 115034 (2016).
- [27] A. Zee, *Phys. Lett.* **93B**, 389 (1980) Erratum: [*Phys. Lett.* **95B**, 461 (1980)]. A. Pilaftsis, *Z. Phys. C* **55**, 275 (1992) [hep-ph/9901206]. L. J. Hall and M. Suzuki, *Nucl. Phys. B* **231** (1984) 419. G. G. Ross and J. W. F. Valle, *Phys. Lett.* **151B** (1985) 375.
- [28] E. Ma, *Phys. Rev. D* **73**, 077301 (2006).
- [29] M. A. Diaz, M. Hirsch, W. Porod, J. C. Romao and J. W. F. Valle, *Phys. Rev. D* **68**, 013009 (2003); Y. Grossman and S. Rakshit, *Phys. Rev. D* **69**, 093002 (2004).
- [30] J. Rosiek, hep-ph/9511250.
- [31] Y. Grossman and H. E. Haber, *Phys. Rev. D* **59**, 093008 (1999); T. F. Feng and X. Q. Li, *Phys. Rev. D* **63**, 073006 (2001).
- [32] B. Dziewit, S. Zajac and M. Zralek, *Acta Phys. Polon. B* **42**, 2509 (2011).
- [33] H. B. Zhang, T. F. Feng, L. N. Kou and S. M. Zhao, *Int. J. Mod. Phys. A* **28**, no. 24, 1350117 (2013).
- [34] T. Asaka, M. Laine and M. Shaposhnikov, *JHEP* **0701** (2007) 091.
- [35] C. Anastasiou, C. Duhr, F. Dulat, E. Furlan, T. Gehrmann, F. Herzog, A. Lazopoulos and B. Mistlberger, *JHEP* **1605**, 058 (2016).
- [36] S. Dodelson and L. M. Widrow, *Phys. Rev. Lett.* **72**, 17 (1994).
- [37] K. Abazajian, G. M. Fuller and M. Patel, *Phys. Rev. D* **64**, 023501 (2001). K. Abazajian, *Phys. Rev. D* **73**, 063506 (2006).
- [38] X. D. Shi and G. M. Fuller, *Phys. Rev. Lett.* **82**, 2832 (1999).